PCCP

Accepted Manuscript

ROYAL SOCIETY OF CHEMISTRY

www.rsc.org/pccp

Tuning the Charge State of Ag and Au Atoms and Clusters Deposited on Oxide Surfaces by Doping. A DFT Study of the Adsorption Properties of Nitrogen- and Niobium-doped TiO_2 and ZrO_2

Philomena Schlexer, Antonio Ruiz Puigdollers, Gianfranco Pacchioni[1]

Dipartimento di Scienza dei Materiali,
Università di Milano-Bicocca, via Cozzi 55, 20125 Milano, Italy

Version: 29.07.2015

Abstract

The charge state of Ag and Au atoms and clusters (Ag_4 and Au_4, Ag_5 and Au_5) adsorbed on defective TiO_2 anatase (101) and tetragonal ZrO_2 (101) has been systematically investigated as a function of oxide doping and defectivity using a DFT+U approach. As intrinsic defects, we have considered the presence of oxygen vacancies. As extrinsic defects, substitutional nitrogen- and niobium-doping have been investigated, respectively. Both surface and sub-surface defects and dopants have been considered. Whereas on surfaces with oxygen vacancies or Nb-doping, atoms and clusters may become negatively charged, N-doping always leads to the formation of positively charged adsorbates, independently of the supporting material (TiO_2 or ZrO_2). This suggests the possibility to tune the electronic properties of supported metal clusters by selective doping of the oxide support, an effect that may result in complete changes of chemical reactivity.

Keywords

Heterogeneous catalysis, nano-catalysis, titania, zirconia, N-doped, Nb-doped, Ag, Au, sub-nanometer clusters, DFT

[1] Corresponding author. E-mail: gianfranco.pacchioni@unimib.it (tel. +39-2644-85219)

Table of contents

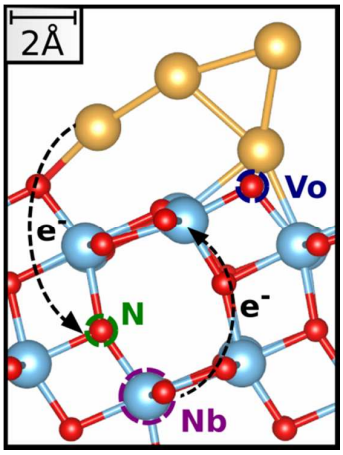

Defects (O vacancies) and dopants (Nitrogen and Niobium impurities) in titania and zirconia affect the properties of adsorbed Ag and Au clusters.

1. Introduction

Noble metal nano-particles supported on oxides show great potential for catalysis and bio-sensing and have therefore been studied extensively in the past.[1,2,3,4,5] To exploit this potential for catalytic applications, detailed knowledge on the catalyst working principle is required and therefore studies aim to determine the mechanisms of reactions catalyzed by supported nano-particles.[6]

The complexity of real catalytic systems makes it difficult to identify the underlying mechanisms on a molecular level. To circumvent this problem, model catalysts can be designed and investigated. So, the contribution of different aspects, such as (electronic) metal-support interaction[7,8], size effects[9,10] and the co-adsorption of molecules that do not directly take part in the reaction[11,12], can be determined. Metal nano-particles can be prepared and deposited on oxides via various methods.[13,14] In some cases, information about the particle size distribution on the support is obtained after deposition, e.g. via STM.[15] Often, the catalytic activity is directly measured after deposition.[16] There is evidence that sub-nanometer clusters and atoms contribute significantly to the catalytic activity of supported Ag and Au clusters[17] for CO oxidation[18,19], the water-gas shift reaction[20] and propylene oxidation,[21,22] just to mention a few examples. The charge state of these nano-catalysts is of fundamental importance to determine their activity.

Titania as support has shown great promoting effects on the catalytic activity of noble metal clusters.[23,24] Many theoretical studies are therefore dedicated to these systems, helping to illuminate the underlying catalytic mechanisms.[25,26,27,28] Under reaction conditions, the active metal component can undergo large morphological changes, such as sintering, which can effectively deactivate the catalyst.[29,30] A possibility to reduce the lateral mass transport could be to anchor the metal particles on the oxide surface via a stronger metal-support interaction. For instance, the presence of oxygen vacancies on titania surfaces is well known to increase the adsorption energy of gold atoms and small clusters on the surface.[31]

Zirconia, on the other hand, is also an insteresting material for catalysis due to its high thermal stability and its mechanical chemical properties for applications as a catalyst support for many reactions.[32] The catalytic properties of zirconia supported metals have been studied experimentally for reactions as the WGS reaction[33], steam reformation of methanol for the production of hydrogen[34] and for the synthesis of methanol from CO_2 and H_2 with Au, Ag or Cu on ZrO_2.[35] Moreover, the Au/ZrO_2 system is of particular interest as a catalyst for CO oxidation.[36,37]

In general, oxide doping is an important strategy to modify the properties of supported catalysts and to stimulate the occurrence of a charge transfer at the metal/oxide interface.[38] There is ample evidence that this can lead not only to changes in the electronic properties of supported metal

particles, but even in their shape.[39,40,41,42] This is the case for instance of Au nanoparticles deposited on Mo-doped CaO films.[39,40] The Mo dopants act as electron donors towards the Au clusters that from neutral and three-dimensional become negatively charged and bi-dimensional. Less frequent is the opposite case, i.e. of a charge transfer from the metal particle to the support. However, the possibility to selectively charge supported nano-clusters represents an interesting way to tune catalytic properties.

In this computational study, we have investigated in a systematic way the effect of intrinsic and extrinsic defects of titania anatase (101) and tetragonal zirconia (101) surfaces on their interaction with small gold and silver clusters. We considered oxygen vacancies (intrinsic defects) and nitrogen- and niobium-dopants (extrinsic defects) in titania and zirconia.

Titania anatase is widely used in catalysis because of its (photo-) catalytic activity as and its promoting effects as support for catalytic applications of metal clusters.[43] The tetragonal phase of zirconia is stable above 1480 K and has excellent mechanical, thermal, chemical and dielectric properties and is therefore of special interest for applications in catalysis.[44,45] Moreover it is possible to stabilize the tetragonal phase under 1480 K by doping with impurities like Mg or Y cations.[46,47]

Nitrogen-doped titania has been the topic of many experimental and theoretical studies, because of the potential use for environmental photo-catalysis.[48] The chemical state of the dopant largely depends on the dopant position[49] (e.g. interstitial or substitutional) and the oxidation state of the host.[50] Di Valentin et al. found that the presence of a nitrogen-dopant can strongly facilitate oxygen vacancy formation on titania.[51] Uncompensated, nitrogen doping introduces an empty acceptor state in the band gap of the hosting oxide (titania and zirconia) (see below). In this study it is mainly used as a dopant with potential to introduce positive charge on adsorbates.

Niobium-doping on the other hand is used to introduce excess electrons in the material. Being a pentavalent ion, Nb substituting Zr or Ti constitutes an electron donor centre. Eben et al. found that Nb doping in titania is favorable even for a fraction of ¼ Nb:Ti.[52] The additional electron introduced by Nb is found to facilitate the adsorption of molecular oxygen on titania,[53] a key step in the CO oxidation reaction. As nitrogen-doping, niobium doping can facilitate oxygen vacancy formation and therefore indirectly affect the cluster adsorption. However, in this study, we will concentrate on the direct effects of the defects on the metal-support interaction and the charge state of the metal clusters, which can have essential consequences for agglomeration behavior and reactivity.

The article is organized as follows. In § 2 we describe the computational approach used. In §

3.1, we will describe shortly the effect of oxygen vacancies, of N- and of Nb-doping on the electronic structure of titania and zirconia surfaces. In § 3.2, we will report on the adsorption properties of atoms and tetramers on stoichiometric and reduced surfaces. Subsequently, we will discuss the effect of nitrogen doping (§ 3.3) and niobium doping (§ 3.4) on the adsorption of atoms and tetramers. In § 3.5 we will consider the adsorption of pentamers on the defective oxide surfaces. In § 4, some conclusion on the findings will be drawn.

2. Computational Details

Periodic, spin polarized density functional theory (DFT) calculations have been performed using the Vienna Ab Initio Simulation Package (VASP 5.2).[54] Generalized gradient approximations (GGA) for the exchange-correlation functional were applied within the Perdew, Burke and Ernzerhof (PBE) formulation.[55]

For transition metal oxides such as TiO_2 and ZrO_2, the GGA approach suffers from the self-interaction error, which significantly affects the electronic structure. To circumvent this error, we used the GGA+U approach as proposed by Dudarev et al.[56] With this approach the multiple occupation of d orbitals is penalized so that the underestimation of the band gap and electron delocalization is attenuated. In this work, we set the U-parameter to 3 eV for the 3d levels of Ti and to 4 eV for the 4d levels of Zr. Also for Nb 4d levels, the U-parameter was set to 4 eV. These parameters provide a good qualitative description of electronic and geometric structures.[57,58,59] We obtain lattice parameters of a_0 = 3.803 Å and c_0 = 9.717 Å for titania anatase and the corresponding experimental values[60] are a_0 = 3.796 Å and c_0 = 9.444 Å. The deviation of the calculated from the experimental unit cell volume is 3.27%. Setting the U-parameter for the Ti 4d levels to 4 eV increases the deviation from the experimental values. This is one argument for using a U-parameter of 3 eV. Another argument is that we aim to calculate the adsorption energies of the metal clusters on the titania surface. A U value of 2-3 eV for the Ti 3d levels has been proposed by Hu et al. to calculate reaction energies on titania.[61] For zirconia, lattice parameters obtained are a_0 = 3.664 Å and c_0 = 5.228 Å. The parameters are in very good agreement with the experimental values[62], showing a deviation of the experimental unit cell volume of less than 1%.

The GGA approach in combination with the PBE exchange-correlation functional does not include dispersion forces. However, these forces may be important for the description of the cluster-support interaction.[63,64] Therefore, we used the semi-empirical dispersion correction as proposed by Grimme known as the DFT-D2 approach.[65] It is generally assumed that the DFT-D2 method produces an overestimate of the dispersion interactions. For this reason we changed the parameters

C_6 and R_0 of the DFT-D2 approach, as suggested by Tosoni and Sauer.[66] We denote this method as DFT-D2' (see also ref. 64). We used this last approach for all the calculations discussed in the following. Considering the bulk lattice parameters, we used those obtained by DFT without vdW-correction. This is justified by the fact that the unit cell volumes of the bulk materials change by much less than 1% (for titania and zirconia, respectively) when the DFT-D2' method is applied with respect to the volume obtained with DFT without dispersion correction.

To describe electron-ion interactions, the projector augmented wave (PAW) method was used.[67] O(2s, 2p), Ti(3s, 4s, 3p, 3d), Zr(4s, 5s, 4p, 4d), Ag(4d, 5s) and Ag(5d, 6s) are described as valence electrons and were consequently treated explicitly. For electronic relaxations, we used the blocked Davidson iteration scheme. [68] In geometric structure optimizations, all ions were allowed to relax until ionic forces are smaller than |0.01| eV/Å. Calculation of the bulk structures were done using a kinetic energy cut-off of 900 eV for TiO_2 and 600 eV for ZrO_2. A Γ-centred K-point grid in the Monkhorst-Pack scheme[69] was used which was set to (8×8×4) for TiO_2 and (8×8×8) for ZrO_2.

To investigate the (101) surface, which is the most stable surface for both materials, we designed slabs with 5 layers of MO_2 (M=Ti or Zr). The slabs were separated by more than 12 Å and all ions were allowed to relax during structure optimizations. We chose a (3×1) surface unit cell for TiO_2 and a (2×2) surface unit cell for ZrO_2. For all subsequent structure optimizations, Γ-point calculations were performed and wave functions were expanded in the plane wave basis up to a kinetic energy of 400 eV. To calculate the projected density of states (PDOS), K-Points were adjusted to (3×3×1). This finer grid was also used to estimate for atomic charges, as described below.

Adsorption energies were calculated as defined in equation (1), where X = Ag, Au and n=1, 4, 5 and M = Ti, Zr. All components refer to structure optimized systems.

$$E_{ADS}\,(X_n/MO_2) = E(X_n/MO_2) - E(X_n) - E(MO_2) \qquad (1)$$

Our unit cells contain 60 Ti or Zr atoms and 120 O atoms, respectively. In the case of titania, we have three different types of oxygen atoms at the surface. All together, the total number of 2-fold coordinated oxygen atoms at the surface is 6 in the (3×1) surface unit cell. Furthermore, there are 12 3-fold coordinated oxygen atoms. Removing one oxygen atom, the concentration of oxygen vacancies is therefore 1/6 or 1/18, depending on the definition. Zirconia shows 8 2-fold coordinated atoms and 8 more O atoms with higher coordination number. For zirconia, the surface

concentration of O vacancies is therefore 1/8 or 1/16. So we have a similar concentration of oxygen vacancies. Nitrogen doping was introduced by substitution of one oxygen; niobium doping by substitution of one Ti (or Zr) atoms. In Fig. 1 we show the positions where the defects or dopants are located. Two different positions of the defects, namely at the surface or at the sub-surface, were considered.

Atomic charges have been estimated with the Bader decomposition scheme.[70] Effective Bader charges are defined as $Q_{eff} = Z_{VAL} - q$, where Z_{VAL} is the number of valence electrons and q is the Bader charge as given by the Bader analysis.

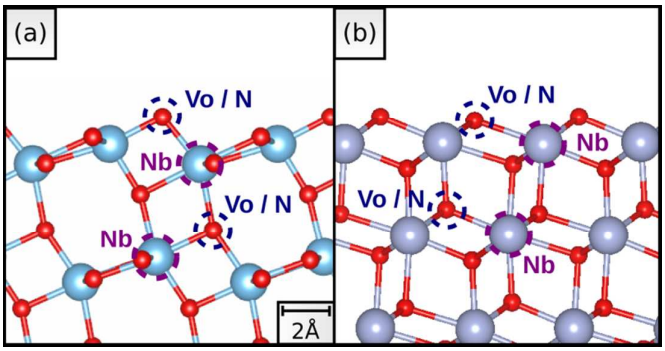

Fig. 1: Positions of defects in (a) titania and (b) zirconia as investigated in this study. For each defect, both surface and sub-surface defects were investigated, respectively. V_O = O vacancy; N = Nitrogen replacing O; Nb = Niobium replacing Ti or Zr.

3. Results and discussion

3.1 Defective titania and zirconia surfaces

Before the adsorption of metal clusters on defective titania and zirconia surfaces will be addressed, a brief summary the effect of the defects on the electronic structure of the systems is given. With the DFT+U approach used we obtain a band gap of 2.6 eV for titania and 4.0 eV for zirconia, smaller than the experimental ones, 3.2 and around 5 eV, respectively.[71,72] The different position of the conduction band minimum (CBM) has essential consequences for the chemistry of the two surfaces. Since the CBM is lower for titania, electrons can be accepted more easily than for zirconia.

The electronic density of states (DOS) of stoichiometric and defective titania and zirconia are shown in Fig. 2. In titania, oxygen vacancies lead to two occupied Ti 3d states in the band gap, Fig. 2 (d). [73,74] The resulting electronic configuration is a triplet. In zirconia, the electrons are singlet coupled and the corresponding state is localized in the vacancy (Vo), Fig. 2 (j).[75] When the vacancy

is on the surface, the defect states can be found a few tenths of an eV below the CBM.

N-doping creates a N 2p empty state in the band gap which in titania does not change much as a function of the location of the dopant (surface or sub-surface). In the case of zirconia, however, the position of the defect state in the band gap changes significantly with the location of N: if N is at the surface, the defect state can be found at around 1 eV above the valence band. When N is sub-surface, the defect state lies only around 0.3 eV above the valence band. The difference in the electronic structure reflects also the difference in stability of the two dopant positions. The surface N-dopant is significantly more stable than the sub-surface one.

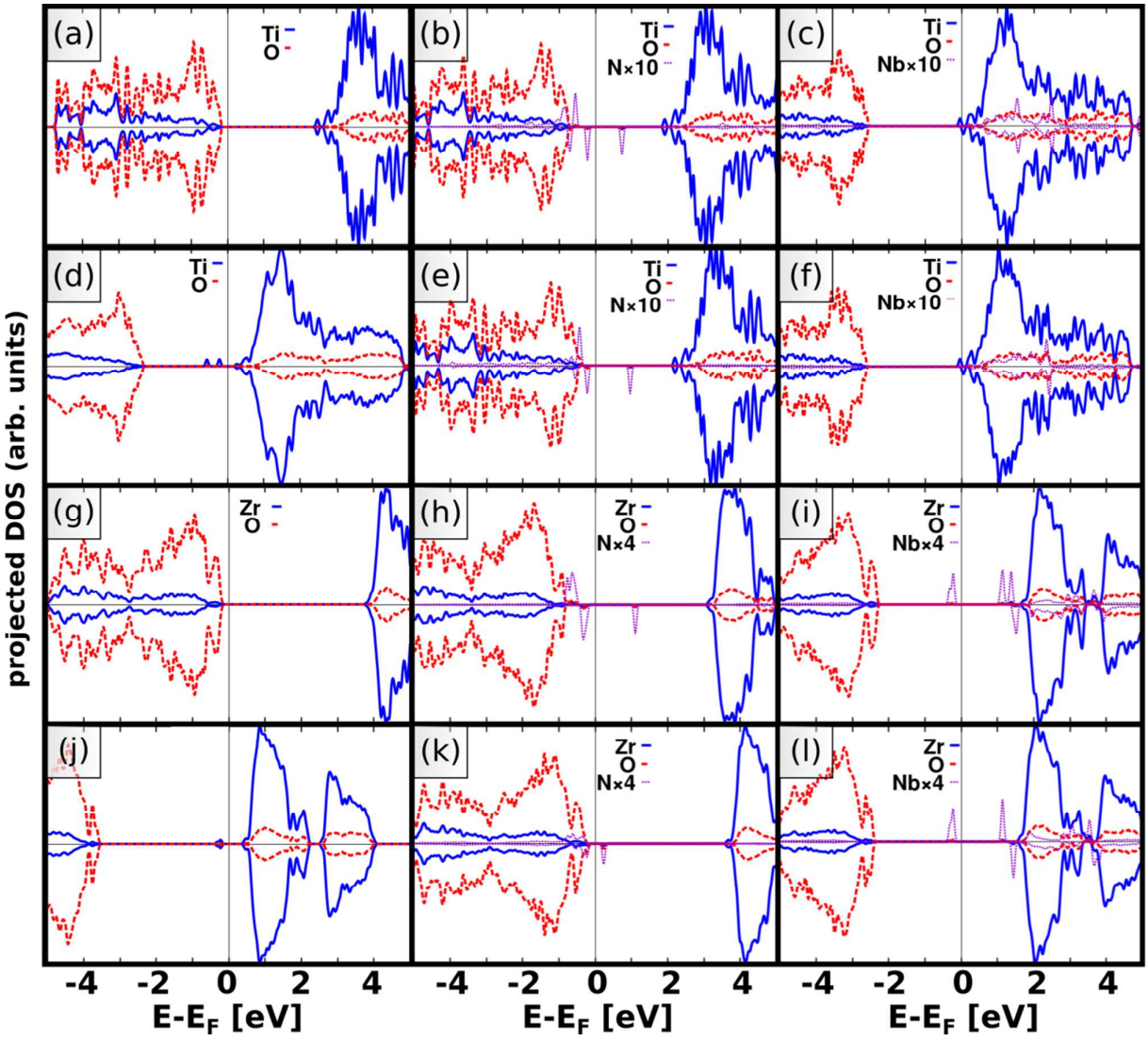

Fig. 2: Projected DOS of (a-f) titania and (g-l) zirconia. (a) Defect-free titania, (b, e) N-doped titania with (b) N at the surface and (e) N at the sub-surface, (c,f) Nb-doped titania with (c) Nb at the surface and (f) Nb at the sub-surface and (d) titania with an oxygen vacancy at the surface. (g) Defect-free zirconia, (h,k) N-doped zirconia with (h) N at the surface and (k) N at the sub-surface, (i,l) Nb-doped zirconia with (i) Nb at the surface and (l) Nb at the sub-surface and (j) zirconia with an oxygen vacancy at the surface. The value of 0 eV corresponds to the Fermi level.

3.2 Ag and Au atoms and clusters on dopant-free surfaces

Ag and Au atoms and clusters have been adsorbed on dopant-free surfaces, i.e. stoichiometric and reduced surfaces of titania and zirconia (101). We will generally discuss first the results for silver and then for gold.

3.2.1 Ag and Au atoms

Silver and gold atoms were adsorbed at different positions of stoichiometric and reduced titania and zirconia. We will show only the thermodynamically most stable cases, for brevity. The resulting adsorption energies, magnetic moments and effective Bader charges are summarized in Table 1.

Table 1: Adsorption energies E_{ads} [eV] magnetic moments μ [μ_B] and effective Bader charges Q_{eff} [|e|] of Ag and Au atoms deposited on stoichiometric and reduced TiO_2 and ZrO_2.

X	Surface	Position (X)	E_{ads} [eV]	|μ|(X) [μ_B]	|μ|(MO_2) [μ_B]	Q_{eff}(X) [|e|]
Ag	TiO_2	2c-O-hollow	-1.04	0.00	0.70	+0.66
	Vo,*surf.*	On Vo, *surf*	-1.94	0.00	0.68	-0.26
	Vo,*sub.*	2c-O-hollow	-1.05	0.00	2.46	+0.66
	ZrO_2	Zr-O-bridge	-0.62	0.19	0.22	+0.01
	Vo,*surf.*	3c-O-hollow	-2.83	0.01	0.48	-0.72
	Vo,*sub.*	Zr-top	-1.13	0.01	0.49	-0.44
Au	TiO_2	5c-Ti-top	-0.61	0.41	0.21	-0.01
	Vo,*surf.*	On Vo, *surf*	-3.07	0.00	0.68	-0.46
	Vo,*sub.*	5c-Ti-top	-1.61	0.00	0.79	-0.43
	ZrO_2	Zr-O-bridge	-1.20	0.38	0.20	-0.16
	Vo,*surf.*	3c-O-hollow	-4.22	0.06	0.46	-0.89
	Vo,*sub.*	Zr-top	-2.43	0.00	0.51	-0.57

Let us first consider the Ag atoms, Fig. 3. The Ag atom adsorbed on the stoichiometric titania surface binds preferentially on a hollow site, Fig. 3 (a) with a relatively large adsorption

energy of -1.04 eV (~0.4 eV more than Au). There is no magnetic moment (no unpaired electron) associated to the Ag atom. However, on the substrate the magnetic moment is 0.7 μ_B. This suggests that the 5s valence electron of Ag has been transferred to the titania substrate. The effective Bader charge of +0.66 |e| on the silver atom is consistent with the idea of a charge transfer from Ag to TiO_2. In the projected electronic density of states, Fig. 4 (a), the empty 5s orbital above the Fermi level and an occupied Ti 3d state can be observed. It can be concluded that a charge transfer occurs and its direction is from the silver to the titania support.

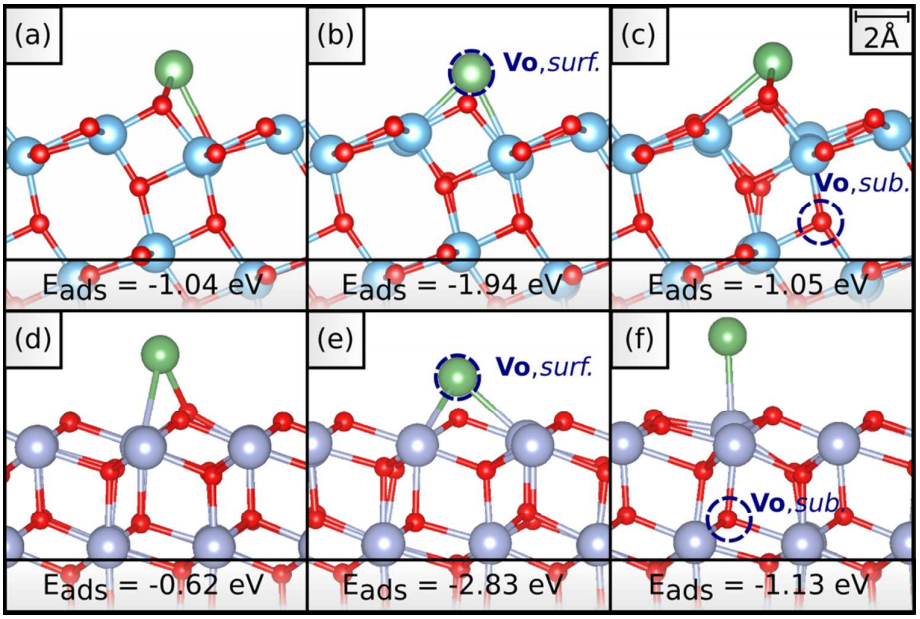

Fig. 3: Positions and adsorption energies of Ag atoms on (a) stoichiometric TiO_2, (b) on TiO_2 with a surface oxygen vacancy (Vo, surf.), (c) on TiO_2 with a sub-surface oxygen vacancy (Vo, sub.), (d) on stoichiometric ZrO_2, (e) on ZrO_2 with a surface oxygen vacancy (Vo, surf.) and (f) on ZrO_2 with a sub-surface oxygen vacancy (Vo, sub.).

The spin density (not shown) shows that the transferred electron is delocalized over the first two layers of Ti atoms, probably a consequence of the use of a small U value in the DFT+U approach. When Ag is positioned on top of a Ti ion, no charge is transferred and the adsorption energy is only around -0.4 eV. However, this is not the global minimum, and therefore it is not relevant for the discussion. We can assume that the higher coordination by oxygen atoms at the 2c-hollow position stabilizes the Ag^+ ion and therefore the charge transfer is facilitated.

Considering the adsorption of the Ag atoms on top of a surface oxygen vacancy, we see that the adsorption energy is enhanced by 0.9 eV, Table 1 and Fig. 3 (b). Again, there is no magnetic

moment on Ag while a value of $\mu(MO_2)$ close to 1 is found on titania, Table 1. This time, however, the effective Bader charge on Ag is negative and the 5s state of Ag is below the Fermi level, Fig. 4 (b). This indicates that the charge transfer is reversed: An Ag^- ion is formed on the surface.

If Ag is deposited above a sub-surface oxygen vacancy, Fig. 3 (c), the obtained parameters are very similar to the case of Ag on the stoichiometric surface, including the charge transfer from Ag to TiO_2. The calculations suggest that a reduction of the Ag^0 adsorbate to Ag^- is only possible if a direct contact between Ti^{3+} ions and the Ag atom can be realised. So, in the case of the sub-surface vacancy, the titania substrate hosts three unpaired electrons per supercell, two from the vacancy and one from the Ag atom which are delocalized over the first two Ti layers.

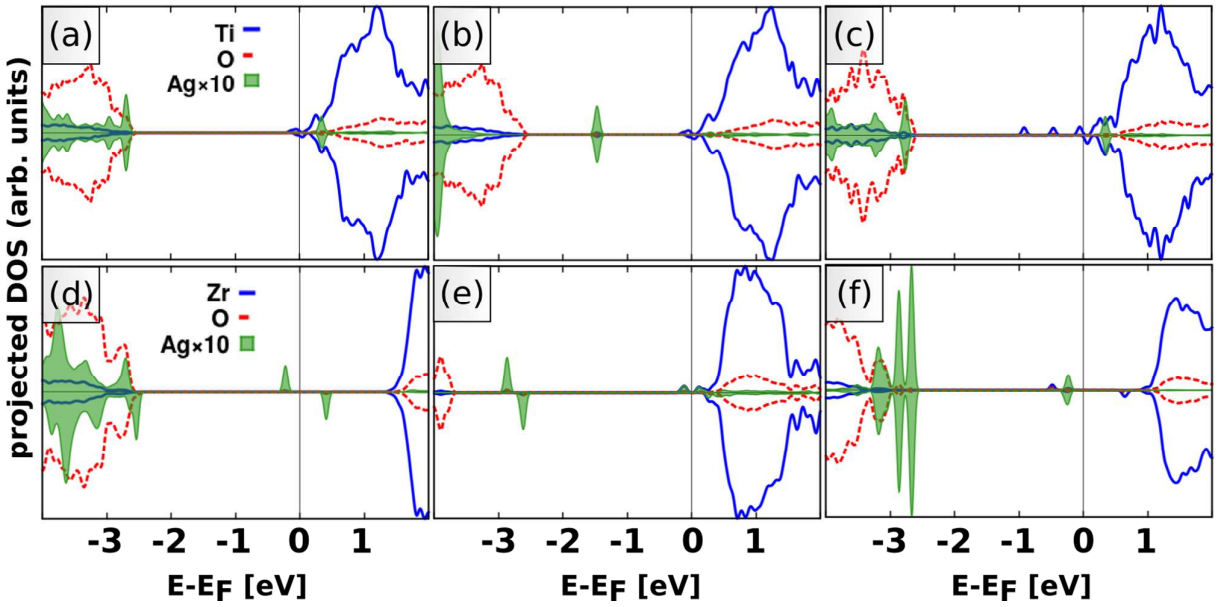

Fig. 4: Projected DOS of Ag atoms on (a) stoichiometric TiO_2, (b) on TiO_2 with a surface oxygen vacancy (Vo, surf.), (c) on TiO_2 with a sub-surface oxygen vacancy (Vo, sub.), (d) on stoichiometric ZrO_2, (e) on ZrO_2 with a surface oxygen vacancy (Vo, surf.) and (f) on ZrO_2 with a sub-surface oxygen vacancy (Vo, sub.).

Let us now consider the Ag atoms on zirconia. On the stoichiometric surface, the Ag atom adsorbs on a Zr-O-bridge site, Fig. 4 (d) with an adsorption energy of -0.62 eV, which is smaller in modulus compared to Ag on stoichiometric titania (-1.04 eV). Considering the DOS, Fig. 4 (d), it can be observed that Ag 5s orbital is half filled indicating an atomic-like configuration, $5s^1$. However, a strong orbital mixing with the surface oxygen atoms leads to a delocalization of the magnetic moment also on the substrate.

As soon as Ag is in direct contact with a surface oxygen vacancy, Fig. 3 (e), the adsorption energy is strongly enhanced, even more than in the case of titania. The charge transfer from the zirconia oxygen vacancy to the Ag atom is confirmed considering the DOS, Fig. 4 (e). In the presence of a sub-surface zirconia oxygen vacancy, Fig. 3 (f), we observe the same bonding mechanism as for Ag on the surface vacancy. This trend is different from that of found for Ag on titania where the charge transfer occurs only when the vacancy is on the surface. So, whereas on titania Ag does not directly interact with the sub-surface vacancy, on zirconia we detect a charge transfer from the support to the Ag atom. This may be a consequence of the fact that the occupied defect states lye at around 3.2 eV above the valence band maximum (VBM) in zirconia, but only at around 1.8 eV above the VBM for titania. The difference of the positions of the defect states reflects the higher reducibility of titania compared to zirconia.

We now consider Au adsorption, Fig. 5, starting also in this case with the titania surface. On stoichiometric TiO_2, Fig. 5(a), Au adsorbs on a 5c-Ti atom with an adsorption energy of -0.61 eV. The metal atom stays neutral and the bonding is due to polarization effects, orbital mixing with Ti and O states and vdW-forces.

On the surface vacancy, Fig. 5 (b) the adsorption energy of Au on titania is enhanced by a factor of five with respect to Au on the stoichiometric surface. The strong bonding is characterized by a charge transfer from Ti^{3+} ions to Au forming Ti^{4+} and Au^{-} species. A low lying completely filled Au 6s orbital can be observed in the projected DOS, Fig. 6 (b). When Au is adsorbed on titania with a sub-surface vacancy, Fig. 5(c), charge transfer in the same direction as for the surface oxygen vacancy can be observed, at variance with Ag. However, the adsorption energy is smaller than for the case where the vacancy is on the surface, Table 1.

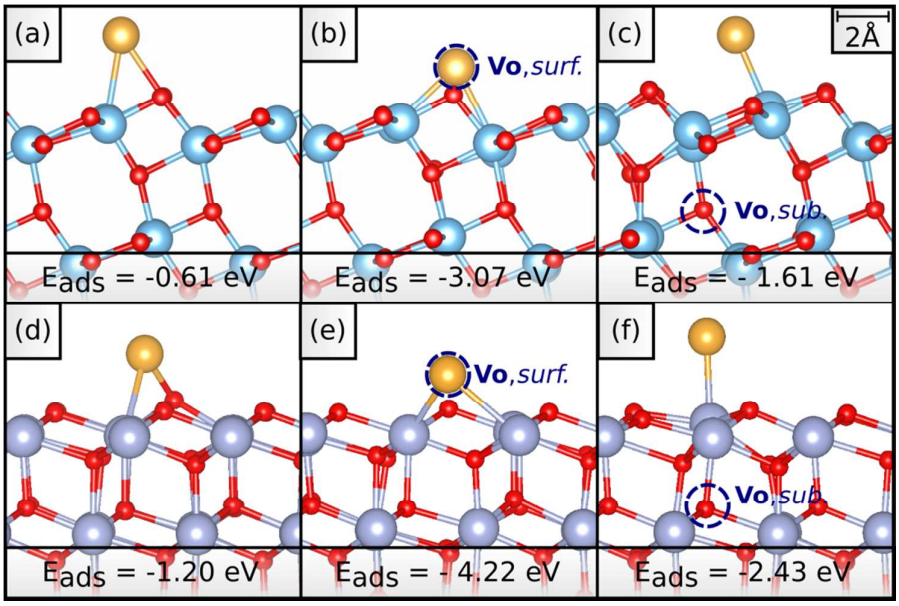

Fig. 5: Positions and adsorption energies of Au atoms on (a) stoichiometric TiO_2, (b) on TiO_2 with a surface oxygen vacancy (Vo, surf.), (c) on TiO_2 with a sub-surface oxygen vacancy (Vo, sub.), (d) on stoichiometric ZrO_2, (e) on ZrO_2 with a surface oxygen vacancy (Vo, surf.) and (f) on ZrO_2 with a sub-surface oxygen vacancy (Vo, sub.).

The enhancement of the adsorption energy in the presence of vacancies will have an important impact on the nucleation and aggregation behaviour of Au on titania.[76] Whereas on the stoichiometric surface, the weak bonding of Au may be accompanied by diffusion of Au atoms and sintering to form larger aggregates, on surface vacancies, Au binds very strong on the vacancy, so that further diffusion on the surface may be inhibited.

Considering Au on zirconia, we can observe essentially the same trend as Au on titania. In general, the adsorption energies of the atoms on zirconia are larger in modulus than on titania, Table 1. The only exception is found for Ag on the stoichiometric surfaces since on titania a net charge transfer bonding occurs, which is not found on zirconia, and which contributes to form a stronger bond.

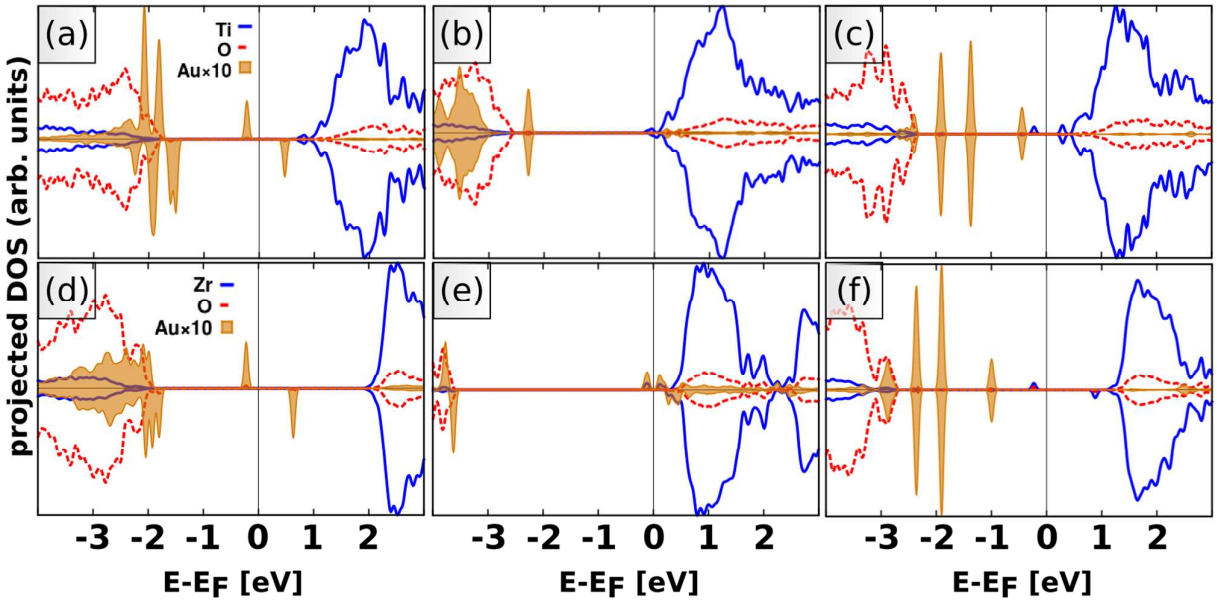

Fig. 6: Projected DOS of Au atoms on (a) stoichiometric TiO_2, (b) on TiO_2 with a surface oxygen vacancy (Vo, surf.), (c) on TiO_2 with a sub-surface oxygen vacancy (Vo, sub.), (d) on stoichiometric ZrO_2, (e) on ZrO_2 with a surface oxygen vacancy (Vo, surf.) and (f) on ZrO_2 with a sub-surface oxygen vacancy (Vo, sub.).

To summarize, we have seen that the presence of oxygen vacancies on titania and zirconia can lead to negatively charged Ag and Au atoms on the surface, which may constitute reactive centres for various reactions. At finite temperatures, it is however expected that metal clusters form by aggregation of individual atoms. For this reason we have investigated Ag_4 and Au_4 clusters. In contrast to the atoms, the tetramers are closed shell systems which may exhibit quite different interactions with the surfaces.

3.2.2 Ag_4 and Au_4 clusters

A significant contribution to the different adsorption properties of atoms or clusters comes from the different ionization potentials (IPs) and electron affinities (EAs). In Table 2, we have summarized the IPs and EAs of the different adsorbates taken from the literature.

Table 2: Ionization potentials and electron affinities [eV] of Ag and Au atoms, tetramers and pentamers.

	Ag	Au	Ag_4	Au_4	Ag_5	Au_5
IP [eV]	7.57[(a)]	9.22[(a)]	5.83[(b)]	7.32[(b)]	5.52[(b)]	6.84[(b)]
EA [eV]	1.30[(a)]	2.31[(a)]	1.63[(a)]	2.56[(a)]	2.12[(a)]	3.06[(a)]

[(a)] Taken from ref.[77], [(b)] taken from ref.[78]

Considering Table 2, we see that the IP values are larger for the atoms than for the clusters. Not surprisingly, IPs as well as EAs are generally higher for gold than for silver. Whereas IPs decrease with increasing cluster size, the EAs increase with increasing cluster size. Based on this information, it may be expected that the atoms show a stronger tendency to remain neutral than the clusters. In the following, we will see if this is actually the case. In this section, we will discuss the adsorption of Ag and Au tetramers on dopant-free surfaces, Table 3. Later, in § 3.5, we will also shortly discuss the adsorption of the pentamers.

In general, the adsorption energies of the tetramers are larger in modulus than for the corresponding atoms. This is not obvious considering that we compare open and closed shell systems. The adsorption energy of Au atom on the surface vacancy of titania (3.07 eV) is for instance only slightly smaller than that of Au_4 (3.45 eV).

Let us first consider Ag_4 on titania. The silver tetramer keeps the structure of a rhombus, lying more or less flat on the surface, Fig. 7 (a). Coordination of the silver atoms occurs mainly with the surface oxygen atoms. On the stoichiometric surface, Ag_4 remains neutral and is bound with an adsorption energy of around -2.0 eV, Table 3. The cluster remains closed shell, see the DOS in Fig. 8 (a). Only a slight orbital mixing with the surface oxygen and titanium atoms can be detected.

Table 3: Adsorption energies E_{ads} [eV], magnetic moments μ [μ_B] and effective Bader charges Q_{eff} [|e|] of Ag_4 and Au_4 clusters deposited on stoichiometric and reduced TiO_2 and ZrO_2 surfaces.

X_4	Surface	E_{ads} [eV]	$\|\|\mu\|(MO_2)$ [μ_B]	$Q_{eff}(X_4)$ [|e|]
Ag_4	TiO_2	-2.02	0.00	+0.36
	Vo,*surf.*	-2.91	0.00	+0.45
	Vo,*sub.*	-2.08	1.71	+0.34

	ZrO_2	-2.17	0.00	0.00
	Vo,*surf.*	-4.30	0.00	-0.95
	Vo,*sub.*	-2.24	0.00	-0.02
Au_4	TiO_2	-2.19	0.00	+0.03
	Vo,*surf.*	-3.45	0.00	-0.82
	Vo,*sub.*	-2.41	1.61	+0.01
	ZrO_2	-3.51	0.00	-0.32
	Vo,*surf.*	-6.18	0.00	-1.22
	Vo,*sub.*	-3.52	0.00	-0.35

When Ag_4 is deposited on titania with a surface vacancy, Fig. 7 (b), the geometric structure changes with respect to the cluster on the stoichiometric surface. Whereas on the stoichiometric surface, the cluster has a rhombic shape, it assumes a Y-shape when deposited on the surface vacancy with two Ag atoms inside the oxygen vacancy.

When the Ag tetramer is deposited on the sub-surface vacancy, Fig. 7 (c), its structure remains like that of the Ag cluster on the stoichiometric surface. In any of these three cases, a charge transfer can be observed, see DOS in Fig 8 (a-c). For Ag_4 on the surface vacancy, mixing of the Ag and Ti 3d orbitals can be observed and as a consequence of the Ag-Ti interaction, the Ti states assume a singlet. The lowest triplet is 0.1 eV higher in energy. For the Ag tetramer on the sub-surface vacancy, the Ti 3d state retains the triplet state, as in the case of the oxygen vacancy without additional adsorbates. In summary, the Ag tetramers remain neutral upon adsorption on stoichiometric and reduced titania.

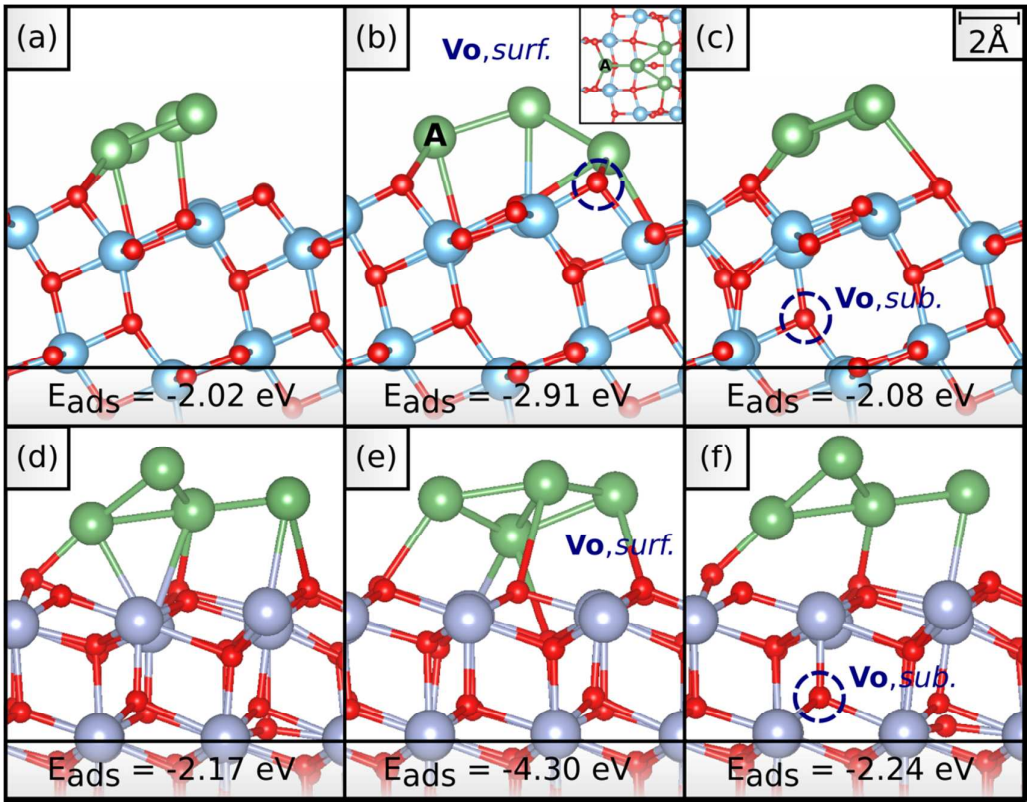

Fig. 7: Structures and adsorption energies of Ag_4 clusters on (a) stoichiometric TiO_2, (b) on TiO_2 with a surface oxygen vacancy (Vo, surf.), (c) on TiO_2 with a sub-surface oxygen vacancy (Vo, sub.), (d) on stoichiometric ZrO_2, (e) on ZrO_2 with a surface oxygen vacancy (Vo, surf.), which is located behind the uppermost middle oxygen atom, and (f) on ZrO_2 with a sub-surface oxygen vacancy (Vo, sub.).

On stoichiometric ZrO_2, Ag_4 assumes a Y-shaped structure, Fig. 7 (d). The cluster remains neutral and closed shell, Fig. 8 (d) and is bound by -2.17 eV, Table 3.

On zirconia with a surface oxygen vacancy, Fig. 7 (e), the cluster geometry changes with respect to that on the stoichiometric surface. Upon deposition on the surface oxygen vacancy, the cluster assumes a rhombic structure. The adsorption energy becomes -4.30 eV, which is much larger in modulus than for the Ag cluster on the stoichiometric surface (-2.17 eV). On the contrary no effect is observed for a sub-surface vacancy where the bonding, -2.24 eV, is similar as on the stoichiometric surface, Table 3. Also the structure, Fig. 7 (f) is similar to that of the stoichiometric surface.

The larger bonding of Ag_4 on the surface vacancy is due to the strong mixing of the Ag_4 with the Vo(ZrO_2) states. On the sub-surface vacancy, instead, less mixing between the states is

found and the binding energy is close to that found on the stoichiometric case, Table 3. The DOS curves, Fig. 8 (d-f), show the absence of electron transfer. This is consistent with the zero magnetic moment of the clusters in all cases. Also the magnetic moment on the substrates is always 0.00 μ_B, except for the subsurface vacancies in titania, Table 3.

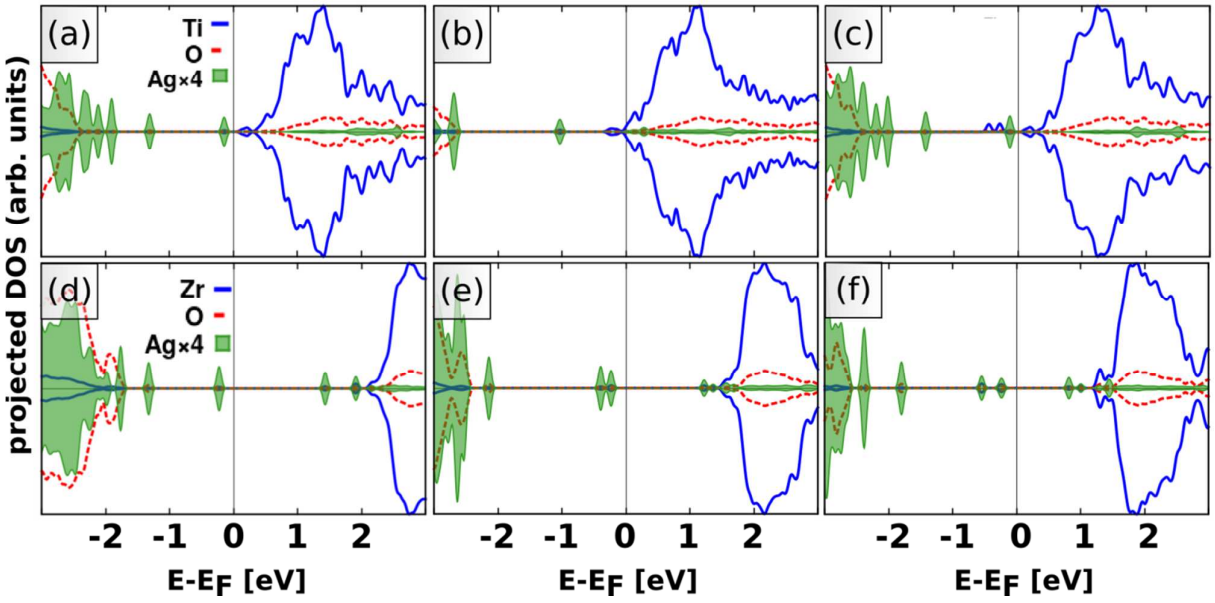

Fig. 8: Projected DOS of Ag_4 clusters on (a) stoichiometric TiO_2, (b) on TiO_2 with a surface oxygen vacancy (Vo, surf.), (c) on TiO_2 with a sub-surface oxygen vacancy (Vo, sub.), (d) on stoichiometric ZrO_2, (e) on ZrO_2 with a surface oxygen vacancy (Vo, surf.) and (f) on ZrO_2 with a sub-surface oxygen vacancy (Vo, sub.).

Considering gold on titania, Fig. 9 (a-c), the tetramers take less flat configurations on titania than the silver tetramers. Gold takes a Y-shape configuration in which one Au atom is pointing towards the vacuum, Fig. 9 (a-c). The adsorption energy of the gold tetramer on the defect-free titania anatase (-2.02 eV) is larger in modulus than the adsorption energy found by Plata et al. (-1.10 eV).[79] This difference is most likely due to the slightly different model and the different treatment of vdW-forces. Whereas we applied the DFT-D2' approach, no vdW-correction was applied in the referred study.

The structure of the Au tetramer does not change significantly going from the stoichiometric surface (Fig. 9 (a)) to the surface vacancy (Fig. 9 (b)) to the sub-surface vacancy (Fig. 9 (c)). As for the Ag_4, also for Au_4 the bonding is stronger on the reduced titania surfaces than on the stoichiometric surface, in particular if the O vacancy is on the surface. From the DOS curves, Fig.

10 (b) a coupling of the gold states with the Ti 3d vacancy states is observed, for the surface oxygen vacancy. The ground state is non magnetic, with the lowest triplet solution 0.1 eV higher in energy, as for the Ag tetramer. Considering the DOS of the sub-surface vacancy, Fig. 10 (c), we can see clearly the two Ti 3d states assuming a triplet. So, as for Ag_4, which is not affected by the presence of a sub-surface oxygen vacancy, also Au_4 is not affected.

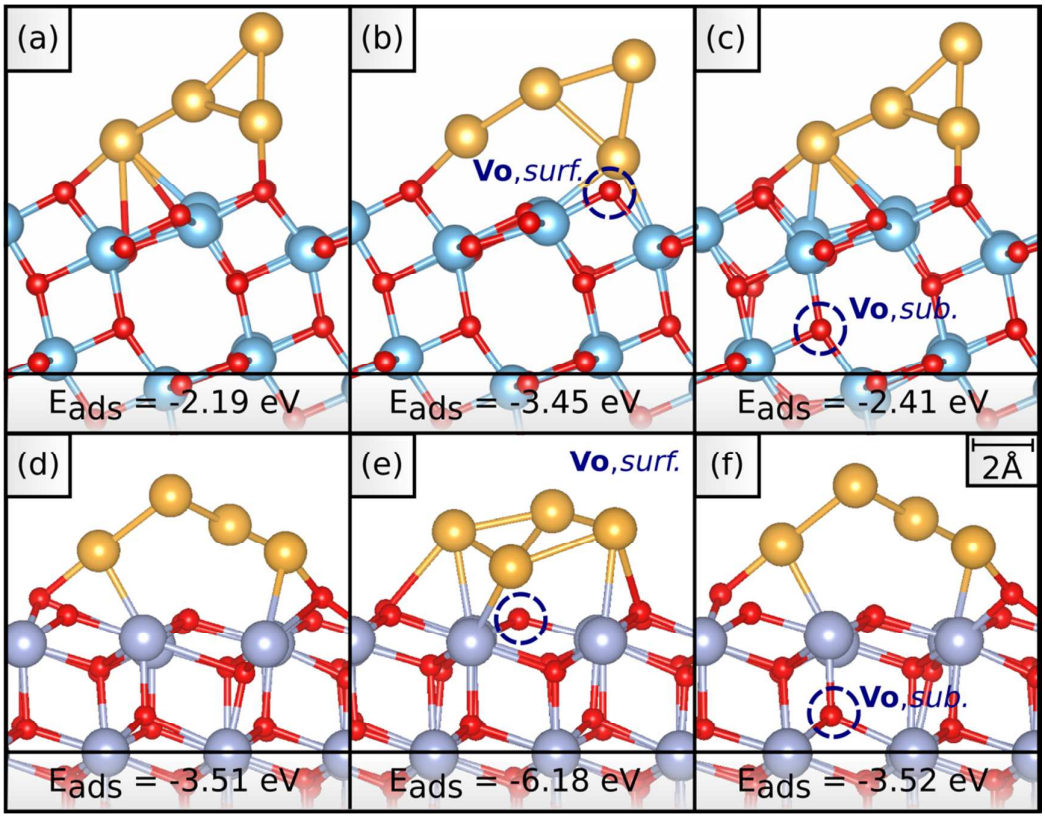

Fig. 9: Structures and adsorption energies of Au_4 clusters on (a) stoichiometric TiO_2, (b) on TiO_2 with a surface oxygen vacancy (Vo, surf.), (c) on TiO_2 with a sub-surface oxygen vacancy (Vo, sub.), (d) on stoichiometric ZrO_2, (e) on ZrO_2 with a surface oxygen vacancy (Vo, surf.) and (f) on ZrO_2 with a sub-surface oxygen vacancy (Vo, sub.).

The optimized structures for Au_4 on stoichiometric and defective zirconia are shown in Fig. 9 (d-f). Similar to Ag_4, the adsorption energy is enhanced in the presence of oxygen vacancies. The binding energy goes from -3.51 eV in the stoichiometric surface to -6.18 eV on the surface vacancy, Table 3. Also in this case the presence of a sub-surface vacancy has no influence, and the adsorption energy (-3.52 eV) remains similar to that of the stoichiometric case. On the surface

vacancy the preferred configuration is a rhombus, Fig. 9 (e), while on the sub-surface vacancy the structure maintains the Y-shape, Fig. 9 (f). The interaction between Au_4 and ZrO_2 is similar to that of Ag_4 with ZrO_2. There is an important mixing of the Au and O ions states in both stoichiometric and defective surfaces, Fig. 10 (d-f), but no charge transfer can be observed.

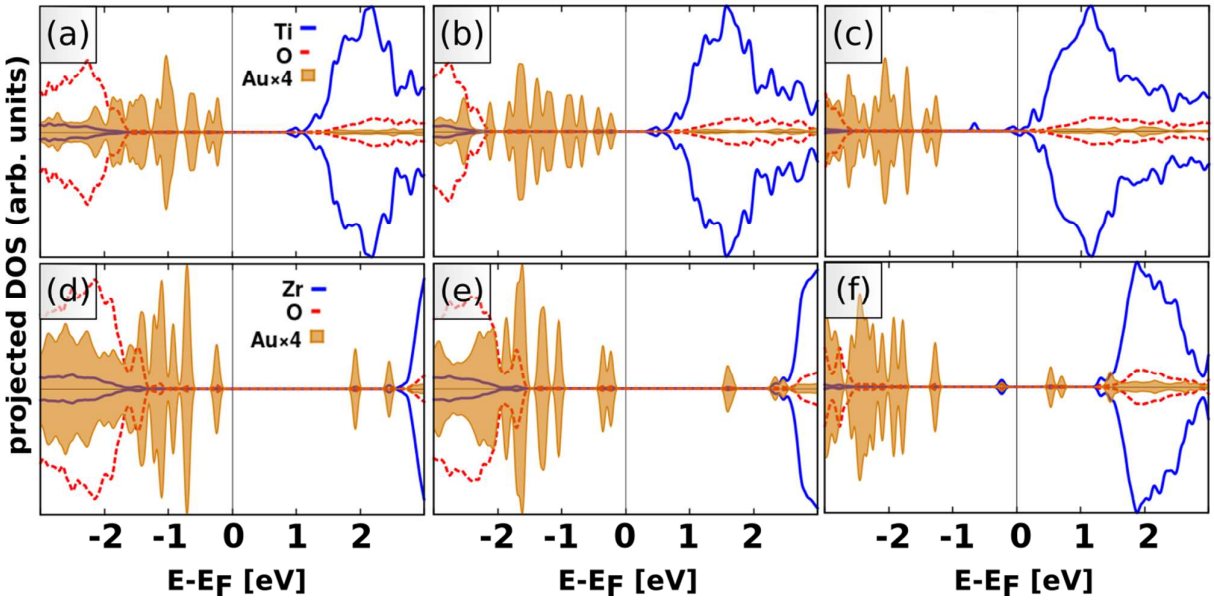

Fig. 10: Projected DOS of Au_4 clusters on (a) stoichiometric TiO_2, (b) on TiO_2 with a surface oxygen vacancy (Vo, surf.), (c) on TiO_2 with a sub-surface oxygen vacancy (Vo, sub.), (d) on stoichiometric ZrO_2, (e) on ZrO_2 with a surface oxygen vacancy (Vo, surf.) and (f) on ZrO_2 with a sub-surface oxygen vacancy (Vo, sub.).

3.3 N-doped a-TiO_2 and t-ZrO_2 surfaces

Nitrogen-doping is an effective method to tune the electronic properties of oxides. We can distinguish at least two ways to introduce a nitrogen dopant in the oxide. If N is substitutional to O, a new singly occupied 2p state appears just above the top of the valence band.[80] The low lying empty 2p component can act as an electron acceptor from higher lying occupied states of adsorbates. If N is interstitial, N-O species form but the electronic structure is similar to that of the substitutional case.[81] Here we concentrate on substitutional N-doping and on the effect it has on the adsorption of Ag and Au atoms and tetramers.

3.3.1 Ag and Au atoms

Silver and gold atoms have been adsorbed on N-doped titania and zirconia, whereby two different positions of the nitrogen dopant have been considered. The N atoms were positioned at the same two places as the oxygen vacancies, i.e. at the surface and at the sub-surface, Fig. 1.

Table 4: Adsorption energies E_{ads} [eV] and effective Bader charges Q_{eff} [|e|] of Ag and Au atoms deposited on N-doped MO_2 (M=Ti, Zr).

X	MO_2	Dopant, position	E_{ads} [eV]	Q_{eff}(X) [|e|]
Ag	TiO_2	N, *surf.*	-3.35	+0.60
		N, *sub.*	-2.89	+0.67
	ZrO_2	N, *surf.*	-2.67	+0.27
		N, *sub.*	-2.97	+0.51
Au	TiO_2	N, *surf.*	-3.01	+0.32
		N, *sub.*	-2.14	+0.45
	ZrO_2	N, *surf.*	-3.14	+0.14
		N, *sub.*	-2.77	+0.29

In Fig. 11, the adsorption positions of Ag and Au atoms on N-doped titania and zirconia are shown. If the N atom is at the surface position, the Ag and Au atoms stay in close contact to it, Fig. 11 (a, c, e, g). On N-doped titania, atoms prefer a hollow site, as the Ag^+ ion on stoichiometric titania, Fig. 3 (a). The only exception of this trend is Au on the surface N-dopant. Here, Au is positioned directly above the N atom, Fig 11 (c).

This position directly above the N-dopant can be observed also for Ag and Au on zirconia when the dopant is on the surface, Fig. 11 (e, g). For the sub-surface N-dopant, the adsorbates are preferentially coordinated by oxygen, Fig. 11 (f, h), as it is also the case for titania.

In general, the adsorption energies of Ag and Au atoms are higher in modulus for N-doped MO_2 than for the stoichiometric and reduced oxides (compare Tables 1 and 4). In no case, a net magnetic moment was found, neither on the noble metal atoms nor on the substrates. The magnetic moment on the tetramers and also on the supports are always 0.00 μ_B. Another observation is that all Bader charges on Ag and Au are positive, Table 4, in contrast to the variety of charge states observed for the non-doped surfaces, Table 1. These features strongly suggest that a charge transfer

from the adsorbates to the low-lying N 2p state occurs.

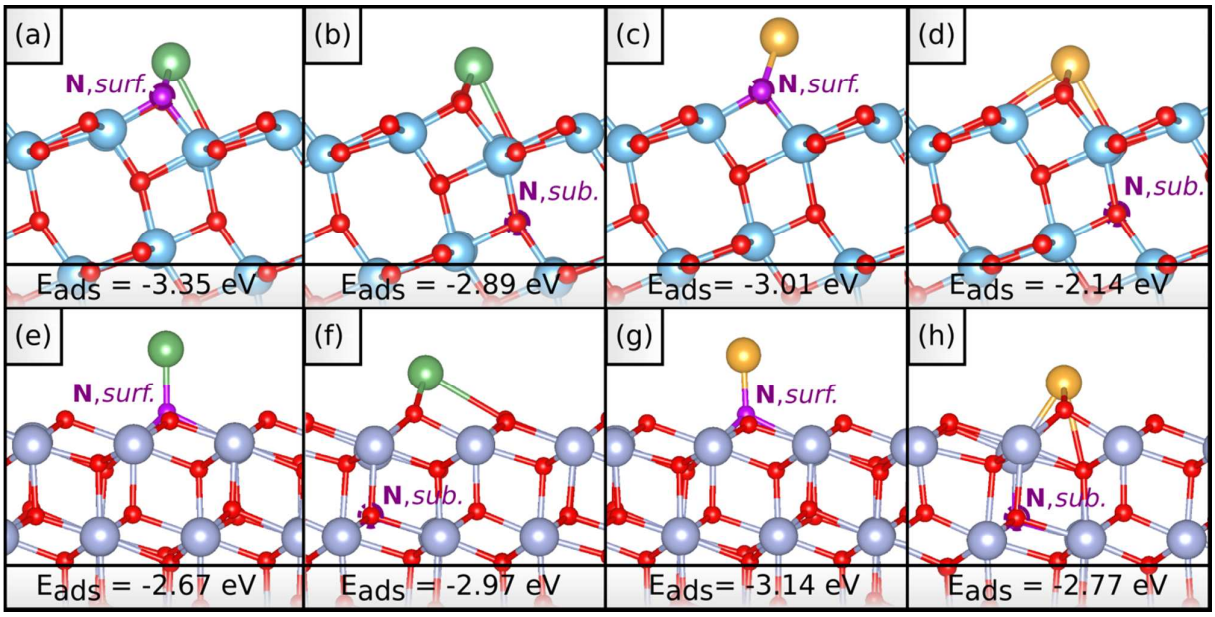

Fig. 11: Positions and adsorption energies of Ag (a,b,e,f) and Au atoms (c,d,g,h) on N-doped titania (a-d) and zirconia (e-h): (a,c,e,g) N at the surface, (b,d,f,h) N at the sub-surface.

The analysis of the DOS curves, Fig. 12, reinforce the conclusions. In each case, the silver 5s state and the gold 6s state are located above the Fermi level, whereas no unoccupied nitrogen state is present in the band gap. The charge transfer from the adsorbates to the nitrogen dopant is confirmed. So, N-doping in both titania and zirconia is able to ionize Ag and Au atoms forming Ag^+ and Au^+ ions.

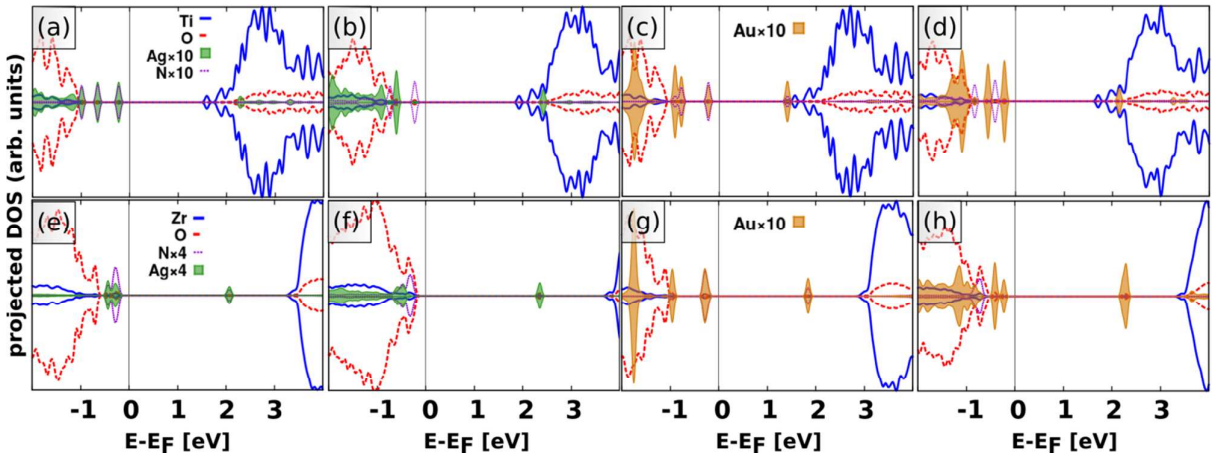

Fig. 12: Ag (a,b,e,f) and Au atoms (c,d,g,h) on N-doped titania (a-d) and zirconia (e-h): (a,c,e,g) N at the surface, (b,d,f,h) N at the sub-surface. Note that in (g), the Nitrogen-projected DOS coincide with the Au-projected DOS.

The acceptor state created by N doping on zirconia is found to be lower in the gap when N is in a sub-surface position, Fig. 2 (k). The gain in energy when one electron fills such state should therefore be larger when the Au and Ag atoms are deposited on the oxide in the presence of sub-surface N-dopants. This behaviour is indeed found for Ag on N-doped zirconia, Table 4. For Au, however, the opposite trend is observed. A higher binding energy is obtained when the atom is adsorbed on N-doped zirconia with the dopant in sub-surface position, Table 4.

3.3.2 Ag_4 and Au_4 clusters

Ag_4 and Au_4 clusters were adsorbed on N-doped titania and zirconia, and the resulting adsorption properties are summarized in Table 5.

Table 5: Adsorption energies E_{ads} [eV], magnetic moments μ [μ_B] and effective Bader charges Q_{eff} [|e|] of Ag_4 and Au_4 clusters deposited on N-doped MO_2 (M=Ti, Zr).

X	MO_2	Dopant, position	E_{ads} [eV]	|μ|(X) [μ_B]	|μ|(MO_2) [μ_B]	Q_{eff}(X) [|e|]
Ag_4	TiO_2	N, *surf.*	-3.82	0.33	0.16	+0.76
		N, *sub.*	-3.56	0.35	0.13	+0.78
	ZrO_2	N, *surf.*	-3.83	0.20	0.16	+0.38
		N, *sub.*	-4.33	0.21	0.17	+0.48
Au_4	TiO_2	N, *surf.*	-3.54	0.52	0.25	+0.29

	N, *sub.*	-2.65	0.60	0.14	+0.49
ZrO_2	N, *surf.*	-4.23	0.34	0.40	-0.19
	N, *sub.*	-4.53	0.50	0.24	+0.18

Considering Table 5, it can be observed that the adsorption energies of the clusters are larger on N-doped substrates compared to the stoichiometric and reduced surfaces, respectively. The geometric arrangements of the clusters, Fig. 13, resemble those found on the stoichiometric surfaces, in particular, the rhombus for Ag_4 (Fig. 13 (a, b, e, f)) and the Y-shape for Au_4 (Fig. 13 (c, d, g, h)).

We observe a non-zero magnetic moment on the clusters, Table 5, which is a first indicator that a charge transfer has occurred since the tetramers have a closed shell ground state when neutral. Considering the effective Bader charges, and keeping in mind the discussion of the previous section, we can conclude that the metal clusters are oxidized by the N-doped substrates.

The magnetic moment on the oxide, which is exactly 1.00 μ_B for the pristine N-doped substrates, decreases upon adsorption of the clusters, while a spin density appears on the metal clusters (0.2-0.6 μ_B, Table 5). One electron is transferred from the HOMO of the cluster to the N-2p level, an effect that can also be observed in the DOS plots, Fig. 14 (a-h)

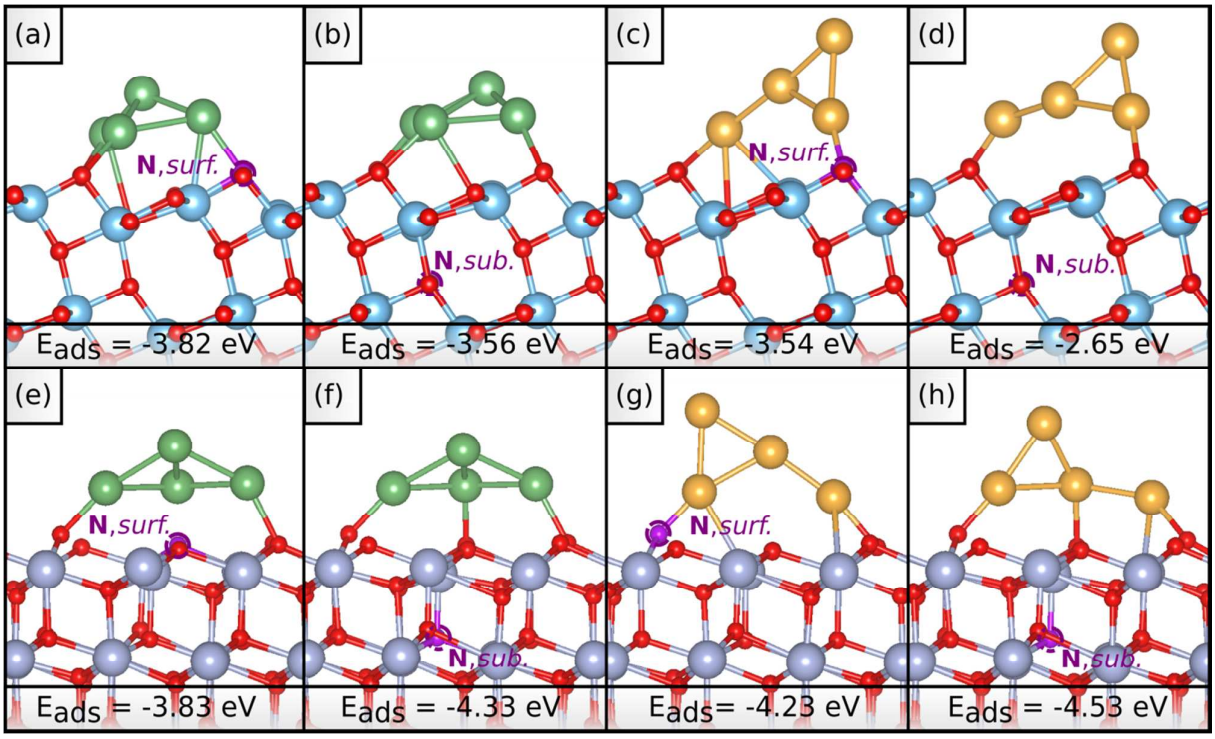

Fig. 13: Structures and adsorption energies of Ag_4 clusters (a,b,e,f) and Au_4 clusters (c,d,g,h) on N-doped titania (a-d) and zirconia (e-h): (a,c,e,g) N at the surface, (b,d,f,h) N at the sub-surface.

On N-doped titania, the bond strength of the clusters is larger when the N dopant is on the surface compared to a sub-surface defect. The direct interaction with the paramagnetic defect results in a strong covalent bonding.

For zirconia similar considerations can be made. However, this time another effect has also to be taken into account. As we have seen before in Fig. 2 (h, k), the empty N 2p states in zirconia have quite different energies when N is at the surface or at the sub-surface. This affects also the adsorption energy of the Ag_4 and Au_4 clusters. Filling the N 2p hole of the sub-surface dopant releases more energy and this results in a stronger bonding.

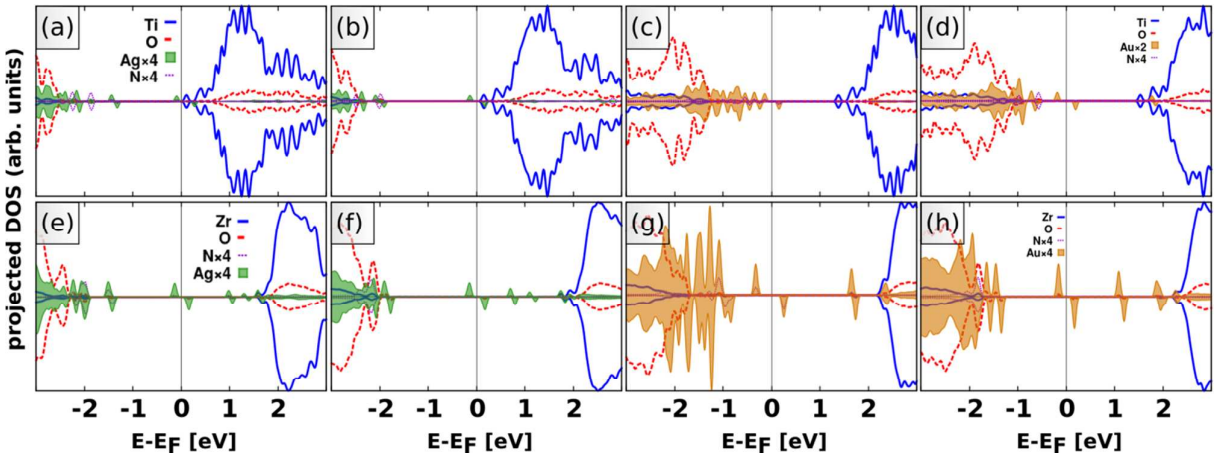

Fig. 14: Projected DOS of Ag_4 clusters (a,b,e,f) and Au_4 clusters (c,d,g,h) on N-doped titania (a-d) and zirconia (e-h): (a,c,e,g) N at the surface, (b,d,f,h) N at the sub-surface.

3.4 Nb-doped a-TiO_2 and t-ZrO_2 surfaces

Nb doping in titania and zirconia can be realized by substituting one Ti or Zr atom by a Nb atom, respectively, or by introducing Nb in interstitial sites. Here we considered only substitutional Nb doping which has different effects on the electronic structures of titania and zirconia. Since Nb has 5 valence electrons, if it replaces the 4-valent Ti or Zr atoms in the lattice it can act as an n-type dopant. However, the effect of introducing Nb in the lattice is completely different for the two oxides. In titania, Nb becomes Nb^{5+} and the excess electron is transferred to the lattice, effectively reducing one Ti^{4+} ion to Ti^{3+}. This means that Nb-doping has a similar effect as creating oxygen

vacancies.[82] In zirconia, however, Nb becomes Nb^{4+} and the fifth valence electron remains localized on a Nb 4d orbital, with no reduction of the oxide. This difference is a direct consequence of the different position of the CBM in the two systems. In the following section, we will see how Nb-doping affects the adsorption of Ag and Au atoms and clusters on the two oxides.

3.4.1 Ag and Au atoms

The adsorption positions and energies of Ag and Au atoms adsorbed on Nb-doped titania and zirconia are shown in Fig. 15. Is Nb positioned at the surface of titania, the atoms prefer to adsorb directly above the Nb atom, Fig. 15 (a, c). Is Nb positioned at the sub-surface, the atoms take the same positions as on the stoichiometric surface, Fig. 15 (b, d), compare Fig. 3 (a) and 5 (a). Ag and Au atoms deposited on Nb-doped zirconia also prefer a position directly above the dopant, when positioned at the surface. For Ag on zirconia with a sub-surface Nb-dopant, an oxygen-hollow position is preferred. Au, on the other hand, keeps a position at the Zr-O-bridge site.

Interestingly, the adsorption energy and the magnetic moments of Ag adsorbed on titania with a surface or sub-surface Nb dopant are exactly the same. However, the effective Bader charge on Ag is negative in the first case and positive in the second case, Table 6. We have seen that when Ag is directly adsorbed on oxygen vacancies it forms Ag^-, while when the vacancy is sub-surface it behaves as on the stoichiometric surface, i.e. it transfers the valence electron to the support with the formation of Ag^+. Given that Nb-doping induces the formation of a Ti^{3+} ion, it is no surprise that we observe the same trend and charge transfer as for the oxygen vacancies.

Table 6: Adsorption energies E_{ads} [eV], magnetic moments μ [μ_B] and effective Bader charges Q_{eff} [|e|] of Ag and Au atoms deposited on Nb-doped MO_2 (M=Ti, Zr).

X	MO_2	Dopant, position	E_{ads} [eV]	$\|\mu\|$(X) [μ_B]	$\|\mu\|$(MO_2) [μ_B]	Q_{eff}(X) [|e|]
Ag	TiO_2	Nb, *surf.*	-0.95	0.00	0.00	-0.25
		Nb, *sub.*	-0.95	0.00	0.00	+0.67
	ZrO_2	Nb, *surf.*	-0.82	0.18	1.26	+0.12
		Nb, *sub.*	-0.53	0.18	1.14	-0.01
Au	TiO_2	Nb, *surf.*	-2.21	0.00	0.00	-0.45
		Nb, *sub.*	-1.52	0.00	0.00	-0.42
	ZrO_2	Nb, *surf.*	-1.17	0.38	1.27	-0.08
		Nb, *sub.*	-0.88	0.37	1.26	-0.13

Considering the DOS, Fig. 16 (a), we can see the completely filled Ag 5s state with a slight mixing between Nb and Ag states. This can be interpreted as the formation of a polar covalent bond between Ag and Nb lying at the surface. The DOS of Ag on a sub-surface Nb-dopant in titania show that the charge transfer is reversed, Fig. 16 (b). The 5s Ag state is above the Fermi level, and two occupied Ti^{3+} $3d^1$ states are present.

On zirconia, the situation for Ag atoms is different. Here, no charge transfer occurs. The excess electron remains localized on the Nb and the Ag atoms remain atomic-like. Also the adsorption energy is similar to that of Ag on the stoichiometric surface (-0.62 eV). When Nb is at the surface, the adsorption energy is slightly enhanced, due to the orbital mixing between Ag and Nb, Fig. 16 (e). When Nb is sub-surface there is neither direct interaction nor charge transfer and the bonding is similar as on the pristine zirconia surface.

Au on Nb-doped titania behaves very similar as Au on titania with oxygen vacancies. In both cases, surface and sub-surface Nb-dopant, Au becomes negatively charged, as it can be seen from the magnetic moments, the Bader charges, Table 6, and the DOS, Fig. 16 (c, d). On Nb-doped zirconia, we find the same features as for Ag on zirconia. The adsorbate remains atomic-like and the excess electron is located at the Nb-dopant. The interaction of the Ag and Au atoms with the defect at the surface results in enhanced adsorption energies compared to the sub-surface Nb-dopant. The direct interaction between adsorbate and dopant at the surface enables strong hybridisation of Nb and Ag or Au states, respectively.

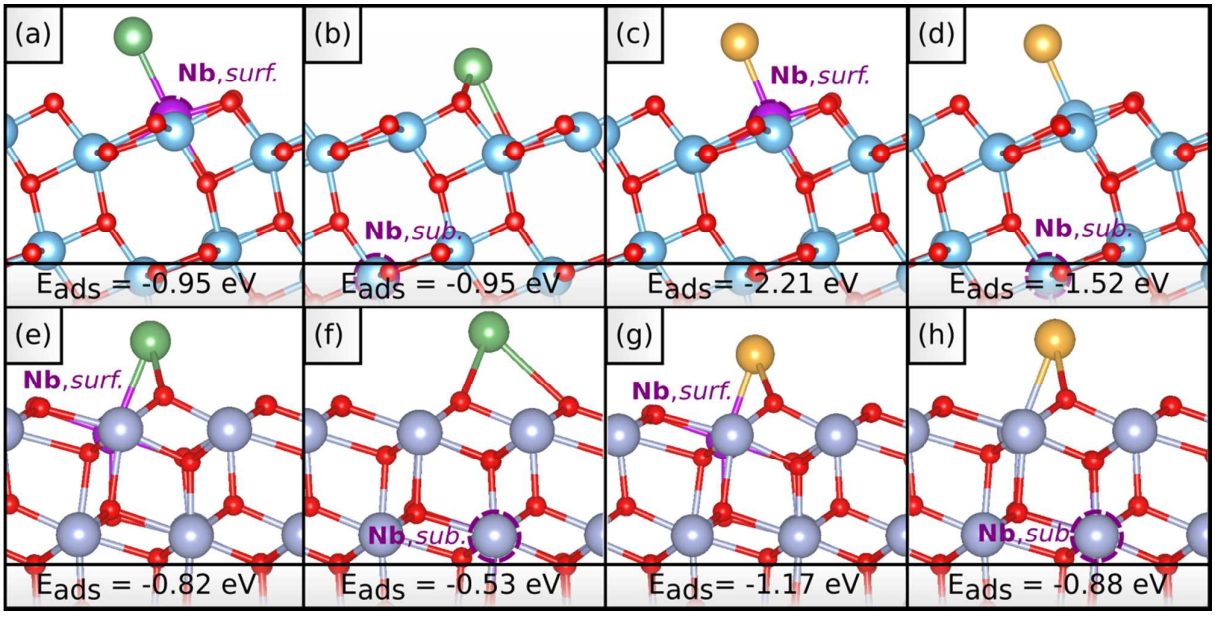

Fig. 15: Positions and adsorption energies of Ag atoms (a,b,e,f) and Au atoms (c,d,g,h) on Nb-

doped titania (a-d) and zirconia (e-h): (a,c,e,g) Nb at the surface, (b,d,f,h) Nb at the sub-surface.

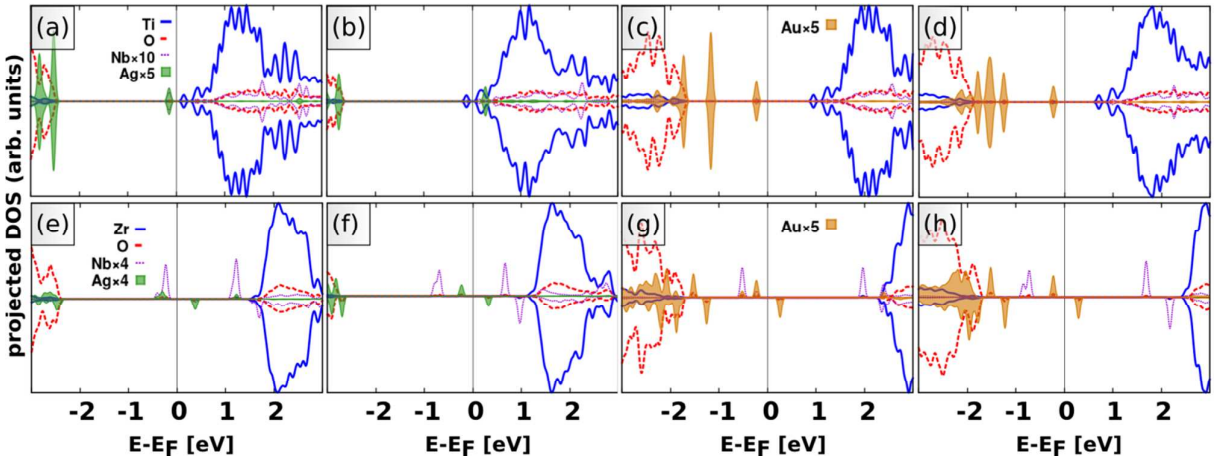

Fig. 16: Projected DOS of Ag atoms (a,b,e,f) and Au atoms (c,d,g,h) on Nb-doped titania (a-d) and zirconia (e-h): (a,c,e,g) Nb at the surface, (b,d,f,h) Nb at the sub-surface.

3.4.2 Ag_4 and Au_4 clusters

Silver and gold tetramers were deposited on Nb-doped titania and zirconia, Table 7 and Fig. 17. The structural properties of the Ag_4 and Au_4 are similar on TiO_2 and Nb-doped TiO_2. The Ag tetramers assume a rhombic structure and the Au tetramers show a Y-shape, Fig. 17 (a-d). A flat Y-shaped structure is taken for Ag and Au tetramers on zirconia with Nb at the surface. The Ag tetramer on the sub-surface Nb-dopant shows a rhombic shape. The Au tetramer shows a Y-shaped geometry.

Considering the adsorption energies, a first interesting observation is that the values are similar to those of the clusters on the stoichiometric surfaces. Furthermore, in all cases the magnetic moments on the metal clusters are zero, indicating the absence of charge transfer.

Table 7: Adsorption energies E_{ads} [eV], magnetic moments μ [μ_B] and effective Bader charges Q_{eff} [|e|] of Ag_4 and Au_4 clusters deposited on Nb-doped MO_2 (M=Ti, Zr).

X	MO_2	Dopant, position	E_{ads} [eV]	|μ|(X) [μ_B]	|μ|(MO_2) [μ_B]	Q_{eff}(X) [|e|]
Ag_4	TiO_2	Nb, *surf.*	-2.33	0.00	0.71	0.34
		Nb, *sub.*	-2.01	0.00	0.69	0.35
	ZrO_2	Nb, *surf.*	-2.37	0.00	0.97	+0.04
		Nb, *sub.*	-1.94	0.00	0.99	0.00

Au_4	TiO_2	Nb, *surf.*	-2.17	0.00	0.00	0.03
		Nb, *sub.*	-2.19	0.00	0.68	0.02
	ZrO_2	Nb, *surf.*	-3.34	0.00	0.99	-0.26
		Nb, *sub.*	-3.12	0.00	0.97	-0.27

More specifically, the adsorption energy for Ag_4 on Nb-doped titania, -2.33 and -2.01 eV for surface and sub-surface dopants, are very close to those of Ag_4 on the stoichiometric surface (-2.02 eV). The DOS curves, Fig. 18 (a,b), confirm the absence of charge transfer for Ag_4 on Nb-doped titania. This is what we found also for the case where the oxide is reduced and oxygen vacancies are present on the surface.

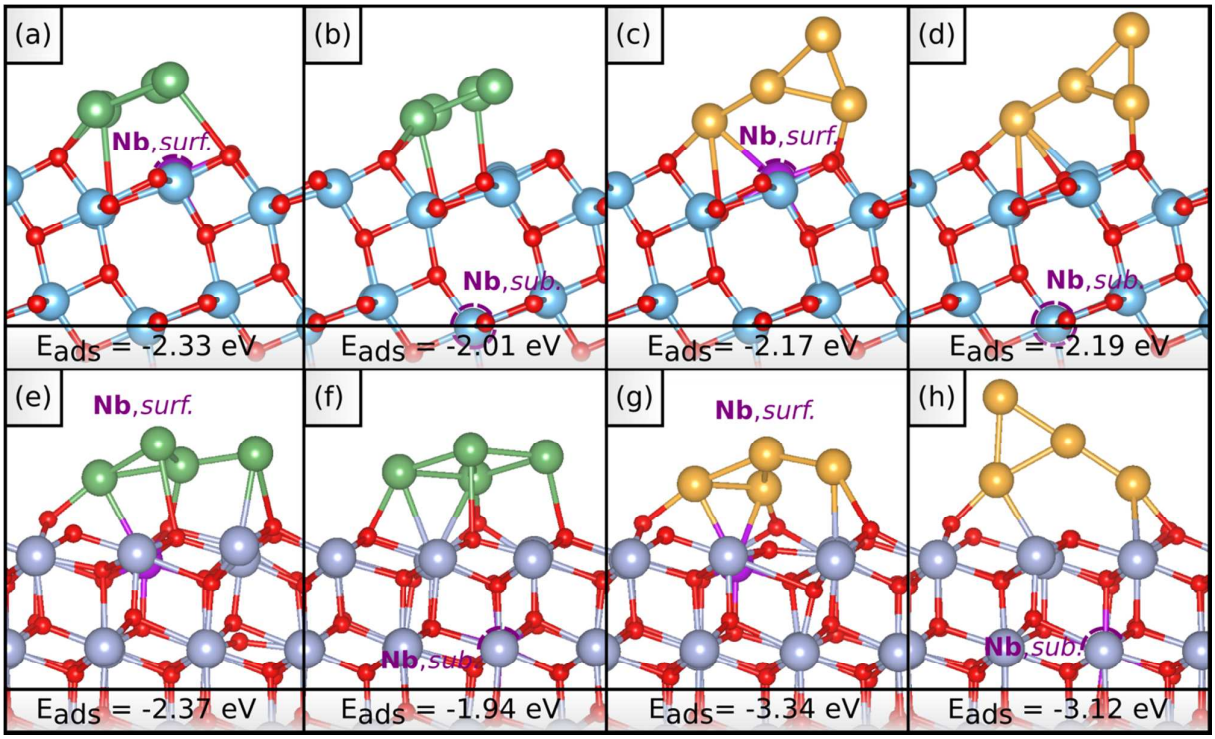

Fig. 17: Structures and adsorption energies of Ag_4 clusters (a,b,e,f) and Au_4 clusters (c,d,g,h) on Nb-doped titania (a-d) and zirconia (e-h): (a,c,e,g) Nb at the surface, (b,d,f,h) Nb at the sub-surface.

Also for Au tetramers on Nb-doped titania the adsorption energies, -2.37 eV and -1.94 eV, Table 7, are very similar as for Au_4 on the stoichiometric surface (-2.19 eV, Table 7). Considering the DOS plots, Fig. 18 (c, d), the occupied Ti 3d state can be seen, a sign that no charge transfer has occurred. In fact, the magnetic moments on the clusters are zero, Table 7. To summarize, the

presence of the Nb dopant has no major effect on the adsorption behaviour of the closed shell Ag and Au tetramers on titania.

Similar considerations can be made for Ag_4 and Au_4 clusters on zirconia. Again a slight enhancement of the adsorption energy can be observed for Ag_4 with respect to the stoichiometric case (-2.17 eV) when the Nb-dopant is at the surface. Au_4 on Nb-doped zirconia exhibits slightly smaller adsorption energies (in modulus) with respect to the stoichiometric case, independent of the location of the Nb dopant, surface or sub-surface. However, the structure of Au_4 on Nb-ZrO_2 (surface dopant) has changed a bit, Fig. 17 (g). Analyzing the DOS, Fig. 18 (g), we can detect a significant mixing of the Au and Nb states, which explains the structural changes: one gold atom approaches Nb and the cluster becomes closer to the surface, Fig. 17 (g).

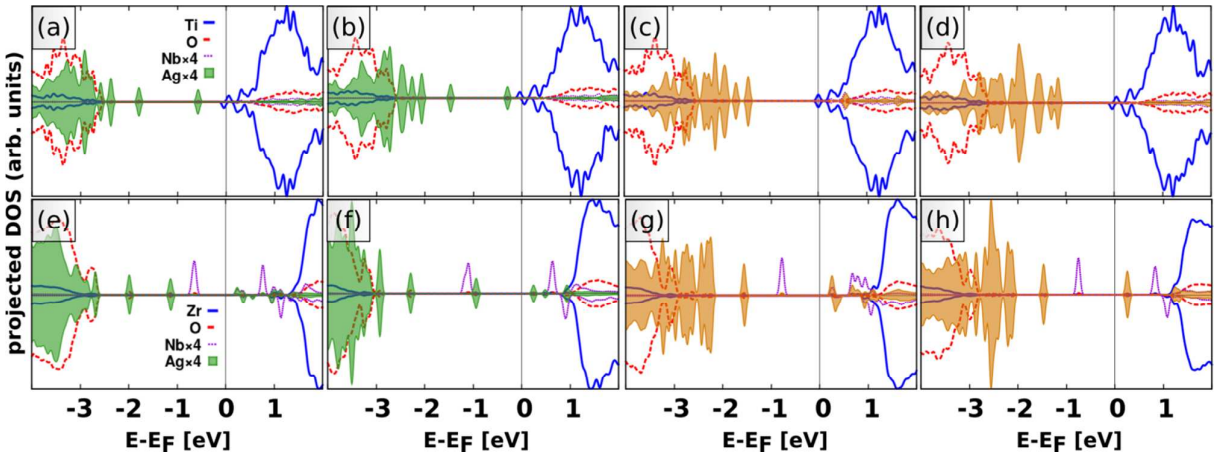

Fig. 18: Projected DOS of Ag_4 clusters (a,b,e,f) and Au_4 clusters (c,d,g,h) on Nb-doped titania (a-d) and zirconia (e-h): (a,c,e,g) Nb at the surface, (b,d,f,h) Nb at the sub-surface.

3.5 What about Ag_5 and Au_5?

In the previous sections, we have seen that in many cases the Ag and Au atoms show different adsorption behaviour than the corresponding tetramers. This is partly the consequence of the fact that the atoms are open shell systems while the tetramers have a singlet closed shell ground state. This raises the question if the pentamers (with an open shell ground state) show a substantially different behaviour than the tetramers. We have therefore investigated Ag_5 and Au_5 on the stoichiometric and defective titania and zirconia surfaces. Oxygen vacancies, N-doping and Nb-doping have been considered. The analysis has been restricted to sub-surface defects, since this is the most general case, Table 8.

On titania the Ag and Au pentamers are quite reactive and tend to transfer one of their

valence electrons to the support, independently on whether there is a defect or not, as we will see in more detail later. Also the kind of defect (O-vacancy, N- or Nb-dopant) does not influence the charge transfer direction. One electron of the pentamer is always transferred to the support with formation of M_5^+ on the surfaces, Table 8.

On zirconia, the situation is similar as for the tetramers, which means that no charge transfer occurs for the stoichiometric surface, for oxygen vacancies and for Nb-dopants. There is only one exception, for Au_5 on the sub-surface oxygen vacancy, where charge transfer from the vacancy to the Au pentamer occurs. This may be a result of the increased EA of the silver pentamers with respect to the tetramers and atoms. On the contrary, on N-doped zirconia the Ag_5 and Au_5 clusters become positively charged, as found for the corresponding tetramers.

Table 8: Adsorption energies E_{ads} [eV], magnetic moments μ [μ_B] and effective Bader charges Q_{eff} [|e|] of Ag and Au pentamers deposited on defective MO_2 (M=Ti, Zr).

X	MO_2	Dopant, position	E_{ads} [eV]	|μ|(X) [μ_B]	|μ|(MO_2) [μ_B]	Q_{eff}(X) [|e|]
Ag_5	TiO_2	Defect free	-2.71	0.00	0.84	0.82
		Vo, *sub.*	-2.59	0.00	2.90	0.81
		N, *sub.*	-4.52	0.00	0.00	0.82
		Nb, *sub.*	-2.64	0.00	0.00	0.81
	ZrO_2	Defect free	-2.05	0.19	0.19	0.00
		Vo, *sub.*	-2.00	0.18	0.21	0.00
		N, *sub.*	-4.84	0.00	0.00	+0.49
		Nb, *sub.*	-1.61	0.20	1.14	0.02
Au_5	TiO_2	Defect free	-1.97	0.00	0.83	0.52
		Vo, *sub.*	-1.77	0.00	0.81	0.51
		N, *sub.*	-3.79	0.00	0.00	0.52
		Nb, *sub.*	-1.89	0.00	0.00	0.52
	ZrO_2	Defect free	-2.84	0.43	0.19	0.00
		Vo, *sub.*	-2.94	0.00	0.51	-0.52
		N, *sub.*	-5.01	0.00	0.00	+0.20
		Nb, *sub.*	-2.63	0.44	1.15	-0.32

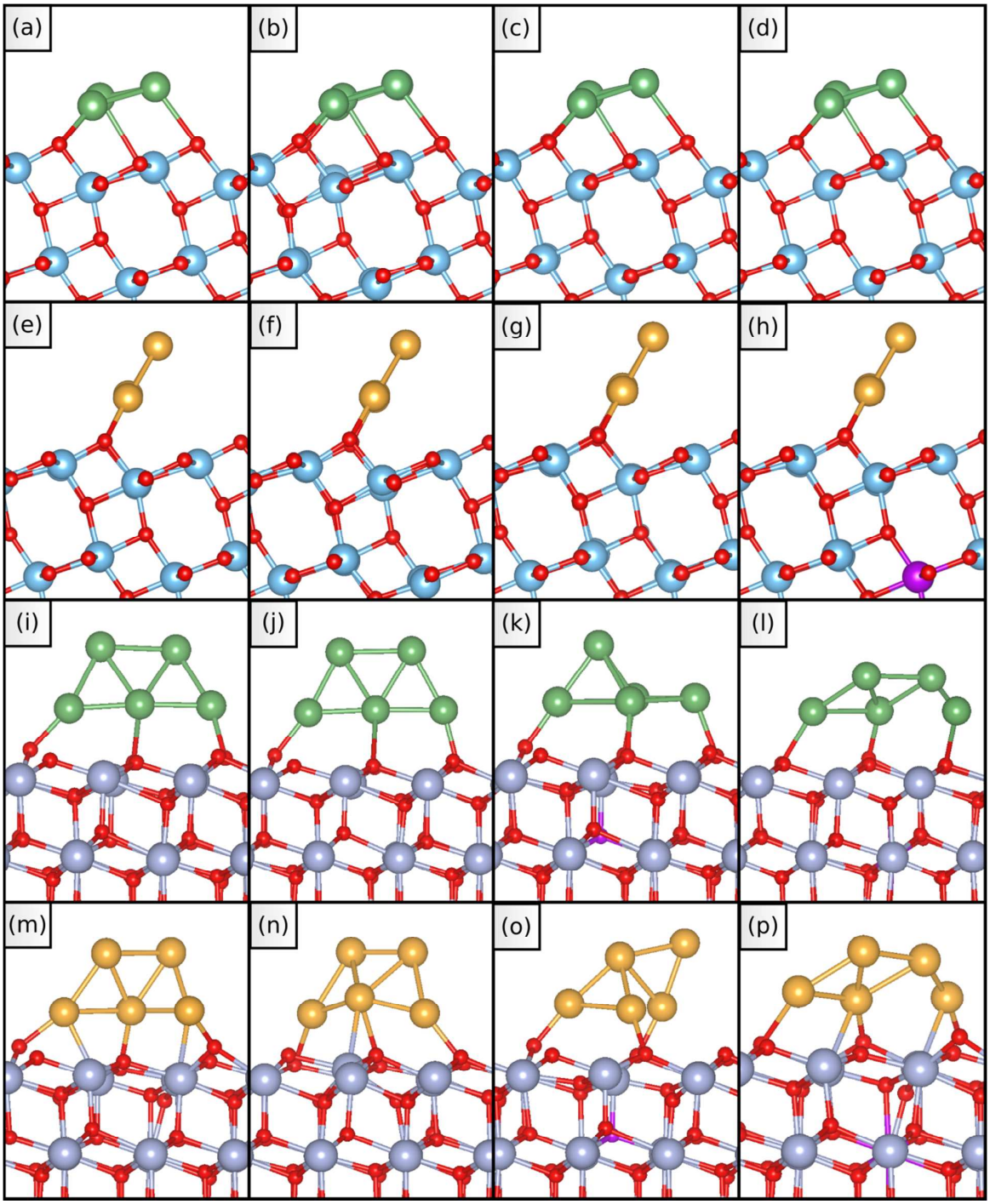

Fig. 19: Structures of Ag and Au pentamers on titania (a-h) and zirconia (i-p) surfaces exhibiting different defects. (a) Ag_5 on the stoichiometric TiO_2 surface, (b) Ag_5 on TiO_2 with a sub-surface oxygen vacancy (Vo, sub.), (c) Ag_5 on TiO_2 with a sub-surface N-dopant (N, sub.), (d) Ag_5 on TiO_2 with a sub-surface Nb-dopant (Nb, sub.). (e) Au_5 on the stoichiometric TiO_2 surface, (f) Au_5 on TiO_2 with a sub-surface oxygen vacancy (Vo, sub.), (g) Au_5 on TiO_2 with a sub-surface N-dopant

(N, sub.), (h) Au_5 on TiO_2 with a sub-surface Nb-dopant (Nb, sub.). (i) Ag_5 on the stoichiometric ZrO_2 surface, (j) Ag_5 on ZrO_2 with a sub-surface oxygen vacancy (Vo, sub.), (k) Ag_5 on ZrO_2 with a sub-surface N-dopant (N, sub.), (l) Ag_5 on ZrO_2 with a sub-surface Nb-dopant (Nb, sub.). (m) Au_5 on the stoichiometric ZrO_2 surface, (n) Au_5 on ZrO_2 with a sub-surface oxygen vacancy (Vo, sub.), (o) Au_5 on ZrO_2 with a sub-surface N-dopant (N, sub.), (p) Au_5 on ZrO_2 with a sub-surface Nb-dopant (Nb, sub.).

The structures for the pentamers on TiO_2 are shown in Fig. 19 (a-h). In general, the pentamers assume a trapeze shape in almost all cases, independently on the support (titania and zirconia). Exceptions are found for the Ag and Au pentamers on N-doped zirconia (sub-surface N-dopant), Fig. 19 (k, o). Considering the pentamers on titania, another general observation is that the Ag pentamers lye more flat on the surface than the Au pentamers. On the other hand, no such difference between Ag and Au pentamers is found for zirconia.

On titania, the presence of the defects does not introduce structural changes with respect to the stoichiometric cases, neither for the Ag pentamers nor for the Au pentamers. Considering the magnetic moments in Table 8 and the DOS in Fig. 3 of the Supplementary Information (a-h), it becomes clear, that this uniform structural trend should be at least partly a consequence of the fact, that the charge state of the pentamers is the same for all cases on titania: Charge transfer occurs from the pentamers to the titania surfaces, forming Ag_5^+ and Au_5^+ ions. This can for instance be seen clearly for the Ag and Au pentamers on the stoichiometric surface, Fig. 3 (a) and (e) of the Supplementary Information. The presence of occupied Ti 3d states in the band gap and empty Ag (or Au) s states above the Fermi level indicate the charge transfer. Similar considerations can be done for the pentamers on the doped surfaces, Fig. 3 of the Supplementary Information (c, d, g, h). The charge transfer behavior is therewith clearly different from that of the tetramers on titania.

Considering the pentamers on zirconia, Fig. 3 of the Supplementary Information (i-p), we can observe that on the stoichiometric surface they remain neutral. On N-doped ZrO_2 there is always a charge transfer from the pentamers to the doped oxide, Fig. 3 of the Supplementary Information (k, o), as it is also the case for the tetramers and atoms on N-doped zirconia. On the contrary, in the presence of a sub-surface oxygen vacancy or a sub-surface Nb-dopant, the Ag and Au pentamers remain neutral, except for the case of Au_5. Here charge transfer occurs from the vacancy to the pentamer, with formation of a negatively charged cluster. The DOS, Fig. 3 of the Supplementary Information, are thus completely consistent with the indications coming from the magnetic moments and the Bader charges, Table 8.

4. Conclusions

In this study we have investigated the effect of oxygen vacancies, N-doping and Nb-doping on the adsorption characteristics of single Ag and Au atoms and small clusters. We found that oxygen vacancies can reduce silver and gold atoms on titania and zirconia, enhancing significantly their adsorption energy with respect to the stoichiometric surfaces. This effect may be exploited to reduce sintering and the negatively charged species can be used to attract and bind electrophilic species, such as O_2 and CO_2. For the tetramers, however, such a charge transfer does not occur. However the adsorption energy is enhanced, especially for the tetramers directly bond to the surface vacancies. Here, the bonding is realized via a covalent polar interaction.

Niobium doping has different electronic effects on titania and zirconia. In titania, Nb substitutional becomes Nb^{5+}, and a Ti^{4+} ion is reduced by the excess electron introduced in the system with formation of Ti^{3+}. In zirconia, the excess electron remains localized at Nb. Niobium doping on the surface results in covalent polar bonds between Ag and Au atoms and Nb. When the dopant is located at the sub-surface, the chemical interaction between the metal adsorbates and Nb is minimized, except in the case of Au on titania, where a charge transfer from Nb to Au occurs. For tetramers, virtually no effect of the Nb-dopant is found neither for either titania or zirconia.

Nitrogen doping induces charges transfer from the Ag and Au adsorbates to the empty N 2p orbital, so that a N^- species is formed. This behavior is found for all Ag and Au adsorbates (atoms, tetramers, and pentamers) on both oxides. The charge transfer is accompanied by an enhancement of the adsorption energies compared to the stoichiometric surfaces. Therefore, N-dopants at or under the surface can act as anchoring points for small Ag and Au clusters. Since the adsorbates become positively charged (oxidized), this can result in a significant change of their chemical properties.

The bonding mechanism of Ag and Au pentamers is different on titania compared to zirconia. Whereas on titania pentamers show a charge transfer to the support, independently on the presence of the defects, they behave similarly as tetramers on defective zirconia where they remain neutral. This is related to the different position of the bottom of the conduction band in the two oxides.

For the atoms, the occurrence of a charge transfer correlates with the trends in ionization potential and electron affinity. For the tetramers and pentamers, on the contrary, the IP and EA do not seem to provide a solid descriptor to predict the charge transfer behavior.

The picture emerging from the present systematic study is rather complex. It shows the potential effect that defects and dopants can have on the electronic and adsorption properties of

metal clusters deposited on oxide surfaces. The occurrence and the direction of a charge transfer can be rationalized a posteriori but is not always easy to predict. It depends on the balance of several factors, and is related not only to the nature of adsorbate and dopant but, for instance, also by their location in the supporting material. Notice that in our analysis we have considered simplified models where the dopants are isolated and do not concur to the formation of other compensating defects (for instance it is known that N doping favors the formation of O vacancies). This shows that dopants in oxide materials and their effect on the properties of supported particles is a complex problem. At the same time it offers a wide range of possibilities to modify the chemistry of supported catalysts.

Acknowledgements

Financial support from the European Marie Curie Project CATSENSE and from the Italian MIUR (FIRB Project RBAP115AYN "Oxides at the nanoscale: Multifunctionality and applications") is gratefully acknowledged. We also thank the COST Action CM1104 "Reducible oxide chemistry, structure and functions".

References

[1] K. An and G. Samorjai, *Catal. Lett*., 2015, **145**, 233
[2] A. West, M. Griep, D. Cole and S. Karna, *Nanotech. Mag. (IEEE)*, 2015, **9**, 25-30
[3] Y. Zhang, X. Cui, F. Shi and Y. Deng, *Chem. Rev.*, 2012, **112**, 2467-2500
[4] T. Takei, T. Akita, I. Nakamura, T. Fujitani, M. Okumura, K. Okazaki, J. Huang, T. Ishida, and M. Haruta, *Adv. Catal*., 2012, **55**, 1
[5] J. Huang and M. Haruta, *Res. Chem. Intermed.,* 2012, **38**, 1
[6] J. A. Rodriguez, J. Evans, J. Graciani, J.-B. Park, P. Liu, J. Hrbek and J. F. Sanz, *J. Phys. Chem. C*, **113**, 7364
[7] M. Bowker and E. Fourre*, Appl. Surf. Sci.,* 2008, **254**, 4225
[8] G. Pacchioni, *Phys. Chem. Chem. Phys.*, 2013, **15**, 1737-1757
[9] M. Shekhar, J. Wang, W. Lee, W. D. Williams, S. Min Kim, E. A. Stach, J. T. Miller, W. Delgass and F. H. Ribeiro, *J. Am. Chem. Soc.*, 2012, **134**, 4700
[10] H. Mistry, R. Reske, Z. Zeng, Z. Zhao, J. Greeley, P. Strasser and B. R. Cuenya, *J. Am. Chem. Soc.*, 2014, **136**, 16473-16476
[11] J. Saavedra, H. A. Doan, C. J. Pursell, L. C. Grabow and B. D. Chandler, *Science,* 2014, **345**, 1599-1602
[12] G. M. Mullen and C. B. Mullins, *Science,* 2014, **345**, 1564-1565
[13] P. Zhao, N. Li and D. Astruc, *Coord. Chem. Rev*., 2013, **257**, 638-665
[14] M. Haruta, *Cattech.*, 2002, **6**, 3
[15] J. Park, S. Conner and D. Chen, *J. Phys. Chem. C*, 2008, **112,** 5490-550
[16] L. Benz, X. Tong, P. Kemper, Y. Lilach, A. Kolmakov, H. Metiu, M. Bowers and S. Buratto, *J. Chem. Phys.*, 2005, **122**, 081102
[17] J. Bokhoven and S. Vajda, *Phys. Chem. Chem. Phys.*, 2014, **16**, 26418
[18] A. Sanches, S. Abbet, U. Heiz, W. D. Schneider, H. Hakkinen, R. Barnett and U. Landmann, *J. Phys. Chem. A*, 1999, **103**, 9573
[19] L. Molina , M. Rassmussen and B. Hammer, *J. Chem. Phys.*, 2004, **120**, 7673
[20] M. Yang, L. Allard and M. Flytzani-Stephanopoulos, *J. Am. Chem. Soc.*, 2013, **135**, 3768
[21] L. M. Molina, S. Lee, K. Sell, G. Barcaro, A. Fortunelli, B. Lee, S. Seifert, R. E. Winans, J. W. Elam, M. J. Pellin, I. Barke, V. von Oeynhausen, Y. Leif, R. J. Meyer, J. A. Alonso, A. F. Rodríguez, A. Kleibert, S. Giorgioi, C. R.

Henryi, K.-H. Meiwes-Broerc and S. Vajda, *Catal. Today*, 2011, **160**, 116-130
[22] Y. Lei, F. Mehmood, S. Lee, J. Greeley, B. Lee, S. Seifert, R. E. Winans, J. W. Elam, R. J. Meyer, P. C. Redfern, D. Teschner, R. Schlögl, M. J. Pellin, L. A. Curtiss and S. Vajda, *Science,* 2010, **328**, 224-228
[23] G. Veith, A. Lumpini, S. Rashkeev, S. J. Pennycook, D. Mullins, V. Schwartz, C. Bridges and N. Dudney, *J. Catal.*, 2009, **262**, 92-101
[24] B. Mao, R. Chang, L. Shi, Q. Zhuo, S. Rani, X. Liu, E. Tyo, S. Vajda, S. Wang and Z. Liu, *Phys. Chem. Chem. Phys*., 2014, **16**, 26645-266652
[25] J. Saavedra, H. Doan, C. Pursell, L. Grabow and B. Chandler, *Science*, 2014, **345**, 1599
[26] L. Liu, B. McAllister, H. Ye and P. Hu, *J. Am. Chem. Soc.*, 2006, **128**, 4017
[27] S. Chretien and H. Metiu, *Cat. Lett.*, 2006, **107**, 143
[28] I. Remediakis, N. Lopez and J. Norskov, *Angew. Chem.*, 2005, **117**, 1858
[29] M. Valden, X. Lai and D. W. Goodman, *Science*, 1998, **281**, 1647
[30] A. Kolmakov and D. W. Goodman, *Surf. Sci. Lett*., 2001, **490**, 597
[31] A. Vittadini and A. Selloni, *J. Chem. Phys.*, 2002, **117**, 353
[32] M. C. Muñoz, S. Gallego, J. I. Beltran and J. Cerda, *J. Surf. Sci. Rep.,* 2006, **61**, 303
[33] V. Idakiev, T. Tabakova, A. Naydenov, Z. Y. Yuan and B. L. Su. *Appl. Catal. B: Environ.,* 2006, **63**, 178
[34] I. Ritzkopf, S. Vukojevic, C. Weidenthaler, J. D. Grunwaldt and F. Schuth, *Appl. Catal. A: Gen.,* 2006, **302**, 215
[35] R. A. Koeppel, A. Baiker, C. Schild and A. Wokaun, *J. Chem. Soc., Faraday Trans.* 1991, **87**, 2821
[36] X. Zhang, H. Wang and B. Q. Xu. *J. Phys. Chem. B,* 2005, **109**, 9678
[37] M. Comotti, W. C. Li, B. Spliethoff and F. Schuth. *J. Am. Chem. Soc.,* 2006, **128**, 917
[38] E. W. McFarland, H. Metiu, *Chem. Rev.*, 2013, **113**, 4391
[39] X. Shao, S. Prada, L. Giordano, G. Pacchioni, N. Nilius and H.-J. Freund, *Angew. Chem. Int. Ed.*, 2011, **50**, 11525-11527
[40] F. Stavale, X. Shao, N. Nilius, H.-J. Freund, S. Prada, L. Giordano and G. Pacchioni, *J. Am. Chem. Soc.*, 2012, **134**, 11380-11383
[41] S. Prada, L. Giordano, G. Pacchioni, *J. Phys. Chem. C*, 2013, **117**, 9943-9951
[42] S. Prada, L. Giordano, G. Pacchioni, *J. Phys. Condens. Matt.*, 2014, **26**, 315004
[43] K. I.Hadjiivanov and D. G. Klissurski, *Chem. Soc. Rev*. 1996, **25**, 61
[44] A. Dwivedi and A. N. Cormack, *Philos. Mag.,* 1990, **61**, 1.
[45] V. V. Kharton, F. M. B. Marqués and A. Atkinson, *Solid State Ionics*, 2004, **174**, 135.
[46] X. Guo, *Phys. Stat. Sol. A*, 2000, **177**, 191.
[47] E. V. Stefanovich, A. L. Shluger and C. R. A. Catlow, *Phys. Rev. B,* 1994, **49**, 11560.
[48] C. Di Valentin, E. Finazzi, G. Pacchioni, A. Selloni, S. Livraghi, M. Paganini and E. Giamello, *Chem. Phys.*, 2007, **339**, 44-56
[49] C. Di Valentin, G. Pacchioni and A. Selloni, *Phys. Rev. B*, 2004, **70**, 085116
[50] C. Di Valentin, G. Pacchioni, A. Selloni, S. Livraghi and E. Giamello, *J. Phys. Chem. B*, 2005, **109**, 11414-11419
[51] S. Livraghi, M. Paganini, E. Giamello, A. Selloni, C. Di Valentin and G. Pacchioni, *J. Am. Chem. Soc.*, 2006, **128**, 15666-15671
[52] E. Dy, R. Hui, J. Zhang, Z. Liu and Z. Shi, *J. Phys. Chem. C*, 2010, **114**, 13162
[53] M. Setvin, U. Aschauer, P. Scheiber, Y.-F. Li, W. Hou, M. Schmid, A. Selloni, U. Diebold, *Science*, 2013, **341**, 988
[54] G. Kresse and J. Hafner, *Phys. Rev. B*, 1993, **47**, 558; G. Kresse and J. Hafner, *Phys. Rev. B*, 1994, **49**, 1425; G. Kresse and J. Furthmuller, *Comp. Mat. Sci.*, 1996, **6**, 15; G. Kresse and J. Furthmuller, *Phys. Rev. B.*, 1996, **54**, 11169.
[55] J. P. Perdew, K. Burke and M. Ernzerhof, *Phys. Rev. Lett.*, 1996, **77**, 3865; J. P. Perdew, K. Burke and M. Ernzerhof, *Phys. Rev. Lett.*, 1997, **78**, 1396.
[56] S. L. Dudarev, G. A. Botton, S. Y. Savrasov, C. J. Humphreys and A. P. Sutton, *Phys. Rev. B*, 1998, **57**, 1505
[57] E. Finazzi, C. Di Valentin, G. Pacchioni and A. Selloni, *J. Chem. Phys.*, 2008, **129**, 154113
[58] J.-H. Lau, L. Wang, S. Li, L.-Y. Yuan, Y.-X. Feng, W. Sun, Y.-L. Zhao, Z.-F. Chai, W.-Q. Shi, *J. Appl. Phys*., 2013, **113**, 183514
[59] O. A. Syzgantseva, M. Calatayud, C. Minot, *J. Phys. Chem. C*, 2012, **116**, 6636
[60] I. Djerdj, A. M. Tonejc, *J. Alloys Compd*, 2006, **413**, 163
[61] Z. Hu and H. Metiu, *J. Phys. Chem. C*, 2011, **115**, 5841
[62] G. Teufer, *Acta. Cryst.,* 1962, **15**, 1187
[63] A. M. Stoneham, *Appl. Surf. Sci.* 1983, **14**, 249-259
[64] A. Ruiz Puigdollers, P. Schlexer and G. Pacchioni, *J. Phys. Chem. C*, 2015, **119**, 15381
[65] S. Grimme, *J. Comp. Chem.*, 2006, **27**, 1787
[66] S. Tosoni and J. Sauer, *Phys. Chem. Chem. Phys.,* 2010, **12**, 14330-14340

[67] P.E. Blöchl, *Phys. Rev. B,* 17953 (1994); G. Kresse, and J. Joubert, *Phys. Rev. B*, 1999, **59**, 1758
[68] E. Davidson, *Methods in Computational Molecular Physics*; Plenum New York, 1983; B. Liu, Report on Workshop "Numerical Algorithms in Chemistry: Algebraic Methods". 1978.
[69] H. J. Monkhorst and J. D. Pack, *Phys. Rev. B*, 1976, **13**, 5188.
[70] W. Tang, E. Sanville and G. Henkelman, *J. Phys. Condens. Matt.*, 2009, **21**, 084204; E. Sanville, S. D. Kenny, R. Smith and G. Henkelman, *J. Comput. Chem.*, 2007, **28**, 899-908; G. Henkelman, A. Arnaldsson and H. Jonsson, *Comput. Mater. Sci.*, 2006, **36**, 254-360
[71] D. O. Scanlon, C. W. Dunnill, J. Buckeridge, S. A. Shevlin, A. J. Logsdail, S. M. Woodley, C. R. A. Catlow, M. J. Powell, R. G. Palgrave, I. P. Parkin, G. W. Watson, T. W. Keal, P. Sherwood, A. Walsh, A. A. Sokol, *Nat. Mater.*, 2013, **12**, 798-801
[72] C. Gionco, M. C. Paganini, E. Giamello, R. Burgess, C. Di Valentin, G. Pacchioni, *Chem. Mater. 2013*, **25**, 2243
[73] H.Y. T. Chen, S. Tosoni and G. Pacchioni, *J. Phys. Chem. C*, 2015, **119**, 10856-10868
[74] M. V. Ganduglia-Pirovano, A. Hofmann and J. Sauer, *Surf. Sci. Rep.*, 2007, **62**, 219-270
[75] S.Fabris, A. T. Paxton and M. W. Finnis, *Acta Mater.*, 2002, **50**, 5171-5178
[76] A. S. Wörz, U. Heiz, F. Cinquini and G. Pacchioni, *J. Phys. Chem. B*, 2005, **109**, 18418-18426
[77] CRC Handbook of Chemistry and Physics, 91st Ed. CRC Press, Boca Raton, 2010
[78] C.W. Bauschlicher, S. Langhoff and H. Partridge, *J. Chem. Phys.*, 1990, **93**, 8133
[79] J. J. Plata, A. M. Márquez, J.F Sanz, R. S. Avellaneda, F. Romero-Sarria, M. I. Domínguez, and J. A. Odriozola, *Top. Catal.*, 2011, **54**, 219-228
[80] C. Di Valentin, G. Pacchioni, A. Selloni, *Phys. Rev. B*, 2004 **70**, 085116
[81] C. Di Valentin, G. Pacchioni, A. Selloni, S. Livraghi and E. Giamello, *J. Phys. Chem. B*, 2005, **109,** 11414–11419
[82] Y. Furubayashi, T. Hitosugi, Y. Yamamoto, K. Inaba, G. Kinoda, Y. Hirose, T. Shimada and T. Hesagawa, *Appl. Phys. Lett.,* 2005, **86,** 252101